Volume 12
Issue 1
July 2023

ISSN - 1857 - 839X

SJCE
SCIENTIFIC JOURNAL OF CIVIL ENGINEERING

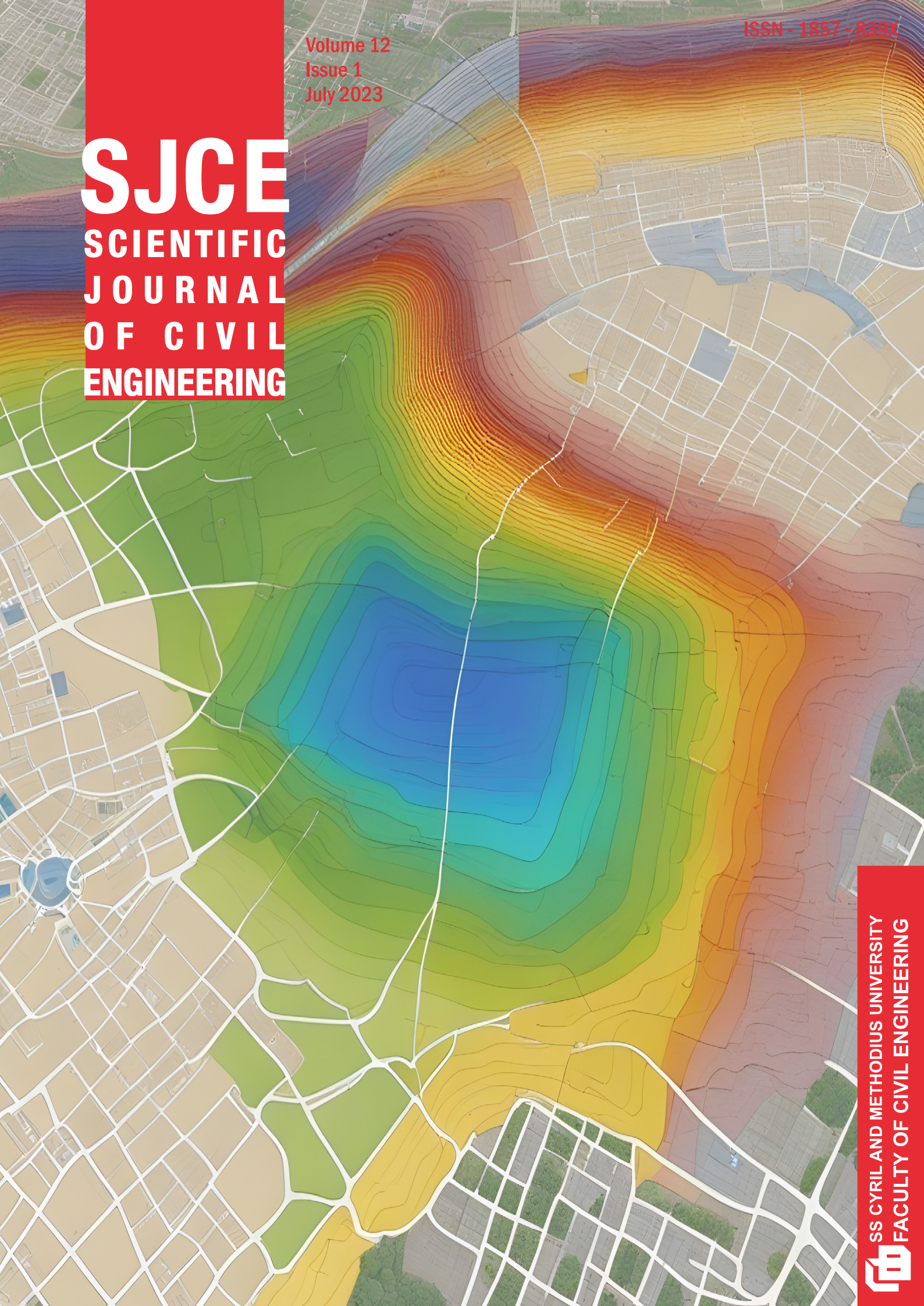

SS CYRIL AND METHODIUS UNIVERSITY
FACULTY OF CIVIL ENGINEERING

EDITORIAL - Preface to Volume 12 Issue 1 of the Scientific Journal of Civil Engineering (SJCE)

Vladimir Vitanov EDITOR - IN - CHIEF

Dear Readers,

The **S**cientific **J**ournal of **C**ivil **E**ngineering (SJCE) is an international, peer-reviewed, open-access journal, initiated in December 2012, and distributed bi-annually. As of December 2021, SJCE has launched its dedicated website and transitioned to a fully digital platform for submission, review, and publication processes. For further details regarding the online edition of the Journal, kindly visit www.sjce.gf.ukim.edu.mk.

At SJCE, we are dedicated to publishing and disseminating high-quality, innovative scientific research across the broad field of engineering sciences. Our journal aims to advance technical knowledge and promote cutting-edge engineering solutions in civil engineering, geotechnics, surveying and geo-spatial engineering, environmental protection, construction management, and related areas. We strive to provide the best platform for researchers to publish their work transparently and comprehensively through our open-access model, offering a forum for original papers that address both theoretical and practical aspects of civil engineering and related sub-topics.

As the Editor-in-Chief of the Scientific Journal of Civil Engineering, it gives me great pleasure to present to you the first Issue of Volume 12, an open-subject edition featuring five scientific research papers that have successfully undergone the established review process of this journal.

These papers cover a range of advanced scientific topics. The first paper evaluates the behavior factor (q-factor) for various configurations of Composite Steel-Concrete Moment Frames using static non-linear analysis, comparing the results with Bare Steel Moment Frames. The second paper discusses the need for repairing and strengthening RC buildings, particularly those damaged by earthquakes or with insufficient construction quality, focusing on the use of innovative materials like CFRP for strengthening RC columns. The third paper outlines the criteria and evaluation process for selecting a new State cartographic projection for the Republic of Macedonia, which is crucial for long-term spatial data quality. The fourth paper aims to assess the flow capacity of Bitola's existing sewer network using EPASWMM, highlighting the evolution of sewer system design from manual calculations to advanced software simulations. The fifth paper presents a study that investigates how climate change impacts the dynamic characteristics of reinforced concrete frame bridges by measuring and comparing their natural frequencies over time. This issue concludes with a tribute paper dedicated to the extensive scientific and academic contributions of Professor Risto Ribaroski, a retired professor from the Faculty of Civil Engineering in Skopje.

The articles in this issue highlight critical advancements in the vast filed of civil engineering, offering valuable insights and practical applications. I genuinely hope that the papers published in this issue will inspire further research in these fields. I extend my gratitude to all the authors for their contributions, and I appreciate the detailed and timely evaluations provided by the reviewers. Lastly, I wish to express my heartfelt thanks to the editorial office members for their remarkable enthusiasm and significant contributions to this journal issue.

Sincerely,

Vladimir Vitanov, Editor-in-Chief

July 2023

SJCE
SCIENTIFIC JOURNAL OF CIVIL ENGINEERING

Impressum

FOUNDER AND PUBLISHER

Faculty of Civil Engineering
Partizanski odredi 24, 1000
Skopje, N. Macedonia

PRINT

This Journal is printed in Mar-saz DOOEL Skopje

EDITORIAL OFFICE

Faculty of Civil Engineering
Partizanski odredi 24, 1000
Skopje, N. Macedonia
tel. +389 2 3116 066
fax. +389 2 3118 834
prodekan.nauka@gf.ukim.edu.mk

EDITOR IN CHIEF

Prof. PhD **Vladimir Vitanov**
Ss. Cyril and Methodius University in Skopje
Faculty of Civil Engineering
Partizanski odredi 24, 1000
Skopje, N. Macedonia
v.vitanov@gf.ukim.edu.mk

EDITORIAL ADVISORY BOARD

Prof. PhD **Valentina Zhileska - Panchovska**
Ss. Cyril and Methodius University in Skopje, Faculty of Civil Engineering, Skopje,
N. Macedonia

Assoc. Prof. PhD **Denis Popovski**
Ss. Cyril and Methodius University in Skopje, Faculty of Civil Engineering, Skopje,
N. Macedonia

Assoc. Prof. PhD **Igor Peshevski**
Ss. Cyril and Methodius University in Skopje, Faculty of Civil Engineering, Skopje,
N. Macedonia

ISSN: 1857-839X

TECHNICAL EDITORS

MSc **Natasha Malijanska Andreevska**
Assistant, Ss. Cyril and Methodius University in Skopje, Faculty of Civil Engineering, Skopje,
N. Macedonia

MSc **Ivona Nedevska Trajkova**
Assistant, Ss. Cyril and Methodius University in Skopje, Faculty of Civil Engineering, Skopje,
N. Macedonia

MSc **Frosina Panovska Georgievska**
Assistant, Ss. Cyril and Methodius University in Skopje, Faculty of Civil Engineering, Skopje,
N. Macedonia

EDITORIAL BOARD

Rita Bento, PhD
Instituto Superior Técnico, Universidade de Lisboa, Department of Civil Engineering, Architecture and Georesources, Lisbon, Portugal

Zlatko Bogdanovski, PhD
Ss. Cyril and Methodius University in Skopje, Faculty of Civil Engineering, Skopje,
N. Macedonia

Heinz Brandl, PhD
Vienna University of Technology, Institute for Geotechnics, Vienna, Austria

Maosen Cao, PhD
Hohai University, Department of Engineering Mechanics, Nanjing, China

Eleni Chatzi, PhD
ETH Zurich, Chair of Structural Mechanics & Monitoring, Zurich, Switzerland

Tina Dasic, PhD
University of Belgrade, Faculty of Civil Engineering, Belgrade,
R. Serbia

Ljupco Dimitrievski, PhD
Ss. Cyril and Methodius University in Skopje, Faculty of Civil Engineering, Skopje,
N. Macedonia

Katerina Donevska, PhD
Ss. Cyril and Methodius University in Skopje, Faculty of Civil Engineering, Skopje,
N. Macedonia

Elena Dumova - Jovanoska, PhD
Ss. Cyril and Methodius University in Skopje, Faculty of Civil Engineering, Skopje,
N. Macedonia

Michael Havbro Faber, PhD
Aalborg University, Department of Civil Engineering, Aalborg, Denmark

Massimo Fragiacomo, PhD
University of L'Aquila, Department of Civil, Construction-Architectural & Environmental Engineering, L'Aquila, Italy

Tomas Hanak, PhD
Brno University of Technology, Faculty of Civil Engineering, Brno, Czech Republic

Nenad Ivanisevic, PhD
University of Belgrade, Faculty of Civil Engineering, Belgrade,
R. Serbia

Milos Knezevic, PhD
University of Montenegro, Faculty of Civil Engineering, Podgorica, Montenegro

SJCE
SCIENTIFIC JOURNAL OF CIVIL ENGINEERING

Impressum

Andrej Kryzanowski, PhD
University of Ljubljana, Faculty of Civil and Geodetic Engineering, Ljubljana, Slovenia

Stjepan Lakusic, PhD
University of Zagreb, Faculty of Civil Engineering, Zagreb, Croatia

Marijana Lazarevska, PhD
Ss. Cyril and Methodius University in Skopje, Faculty of Civil Engineering, Skopje, N. Macedonia

Peter Mark, PhD
Ruhr University, Faculty of Civil and Environmental Engineering, Bochum, Germany

Marc Morell
Institute des Sciences de l'Ingénieur de Montpellier, France

Vlastimir Radonjanin, PhD
University of Novi Sad, Faculty of Technical Sciences, Novi Sad, R. Serbia

Marina Rakocevic, PhD
University of Montenegro, Faculty of Civil Engineering, Podgorica, Montenegro

Resat Ulusay, PhD
Hacettepe University, Faculty of Engineering, Ankara, Turkey

Joost C. Walraven, PhD
Delft University of Technology, Department of Civil Engineering, Delft, Netherlands

Zlatko Zafirovski, PhD
Ss. Cyril and Methodius University in Skopje, Faculty of Civil Engineering, Skopje, N. Macedonia

Ales Znidaric, PhD
ZAG – Slovenian National Building and Civil Engineering Institute, Ljubljana, Slovenia

ORDERING INFO

SJCE is published bi-annually.
All articles published in the journal have been reviewed.

Edition: 100 copies

SUBSCRIPTIONS

Price of a single copy:
for Macedonia (500 den);
for abroad (10 EUR + shipping cost).

BANKING DETAILS (NORTH MACEDONIA)

Narodna banka na RNM
Account number:
160010421978815
Prihodno konto 723219,
Programa 41

BANKING DETAILS (INTERNATIONAL)

Correspond bank details:
Deutsche Bundesbank Zentrale
Address: Wilhelm Epstein Strasse 14 Frankfurt am Main, Germany
SWIFT BIC: MARK DE FF
Bank details:
National Bank of the RNM
Address: Kompleks banki bb 1000 Skopje, North Macedonia
SWIFT BIC: NBRM MK 2X
IBAN: MK 07 1007 0100 0036 254
Name: Gradezen fakultet Skopje

SELECT A PROFESSION

CREATIVE	SOPHISTICATED	RECOGNIZED	RESPONSIBLE
ENDURING	UP-TO-DATE	WORLWIDE	IMPORTANT

WWW.GF.UKIM.EDU.MK

OUR FACULTY CAN GIVE YOU

IMPULSE !	SCHOLARSHIPS FOR THE BEST	ASSURANCE !	COORPERATION WITH INDUSTRY AND INTERNATIONAL UNIVERSITIES
SIMPLE ENROLLMENT	MOTIVATION !	100% EMPLOYMENT AND INTERNATIONALLY RECOGNIZED DIPLOMA	SUPPORT !

WWW.GF.UKIM.EDU.MK

SJCE
SCIENTIFIC JOURNAL OF CIVIL ENGINEERING

CONTENTS

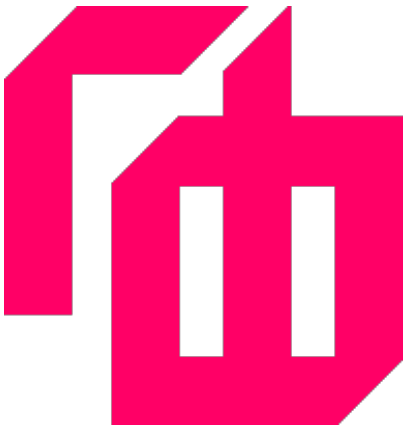

СЕКОГАШ БИДИ ИН

WWW.GF.UKIM.EDU.MK

Denis Popovski
PhD, Associate Professor
Ss. Cyril and Methodius University in Skopje
Faculty of Civil Engineering
N. Macedonia
popovski@gf.ukim.edu.mk

Mile Partikov
PhD, Assistant Professor
Ss. Cyril and Methodius University in Skopje
Faculty of Civil Engineering
N. Macedonia

Ditar Memedi
MSc in Civil Engineering
Ss. Cyril and Methodius University in Skopje
Faculty of Civil Engineering
N. Macedonia

COMPARATIVE STUDY ON BEHAVIOUR FACTOR FOR COMPOSITE AND BARE STEEL FRAMES

One of the basic parameters for dynamic analysis of structures according to modern design regulations is the behavior factor, i.e. the q –factor. For different types of structural system configurations and ductility classes, in Eurocode 8, upper limits for this parameter are given. When it comes to Composite Steel-Concrete Frames, results in this area are relatively limited.

In this paper, using a static non-linear analysis, an evaluation of the q –factor has been performed for different types of configurations of Composite Steel-Concrete Moment Frames (Composite Frames). The individual components that make up the q-factor are determined, and their variations are interpreted depending on the frame configuration. The influence of specific parameters, such as the span and number of stories of the frame, and member local characteristics are studied. The geometrical and material nonlinearity of composite cross sections are taken into account with the concept of distributed plasticity. The obtained results are compared with the proposed values for Bare Steel Moment Frames.

Keywords: behavior factor, steel-concrete moment frames, steel frames, nonlinear static analysis

1. INTRODUCTION AND MAIN CONCEPTS

While analyzing structures under the influence of seismic dynamic loads, one of the main difficulties is to describe the behavior of the system outside the elastic region. Seismic codes, such as Eurocode 8 [7], ASCE [11], etc., recommend the use of simplified methods based on elastic linear analysis. The philosophy of treating structures affected by seismic inertial forces is based on the following formulation: Seismic forces obtained from the elastic response spectrum are reduced at the cost of the dissipative capacity of the structure [12]. In other words, part of the seismic forces is received by the construction with elastic behavior, while with the remaining part of the seismic force, the structure behaves non-linearly. To what extent the construction can

behave linearly (and non-linearly, respectively), in principle depends on many parameters. Namely, all parameters are accumulated and (to a certain degree of precision) described by the q-factor. The recommended values of this factor are used, which are attached in Eurocode 8[14], Table 6.2. The tabular values for the q-factor are given for steel frames, and there are no additional provisions when instead of bare steel beam, a composite one is chosen. In this paper, during the analysis and quantification of the q-factor, the following parameters are considered: the number of levels and the span of the frame; the "column/beam" capacity ratio (the "strong columns/weak beams" criterion); the plastic rotation capacity of the columns; the ratio of permanent to variable loads (N/Np). This principle is used in the analysis of both the composite and bare steel moment frames. The obtained values are compared with those recommended by Eurocode 8, so the possible consequences of this choice of the q-factor are subject to discussion.

2. METHODOLOGY OF CALCULATING THE BEHAVIOUR FACTOR

The determination of the q-factor - for both steel and the composite frames - a Pushover analysis was carried out, with a monotonically incremental increase in the equivalent seismic horizontal force, with the gravity loads (in the seismic combination) being constantly present during the entire procedure. In this paper, the horizontal load is applied with a triangular shape, while the analysis is carried out with the SeismoStruct 2018 software package.

The segment bounded by points O-B describes the linear-elastic behavior, up to the limit of occurrence of the first plastic hinge (point B). The corresponding displacement at the occurrence of the first plastic hinge is denoted with Δ_y, it marks the beginning of the second phase of the monotonically increasing F-Δ curve. This part of the curve is generated as a result of the plastic capacity for the redistribution of internal forces, until reaching the ultimate state (point C), at a corresponding displacement Δ_{F_u}.The part bounded by the C-E curve is called the softening branch [9] and it dependent on the type of fracture mechanism and the intensity of the vertical loads. To determine the q-factor, the formulation according to [1] is used in this paper. The q-factor is determined as a product of the three parameters that are responsible for the dynamic behavior of a certain structural system, that is: R_Ω –design reserve strength; R_μ –ductility factor and R_ρ –redundancy factor.

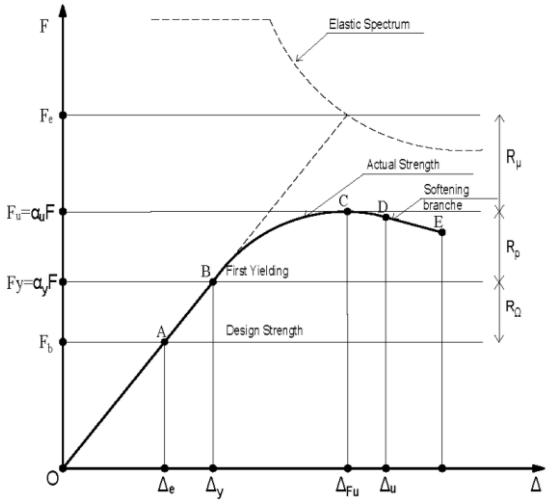

Figure 1. Typical pushover curve [1].

2.1 PERFORMANCE LIMITS ACCORDING TO FEMA 356

The nonlinear behavior of plastic hinges is described according to FEMA 356 criteria [3]. For this purpose, the force-deformation dependence is used, as in Figure 2.

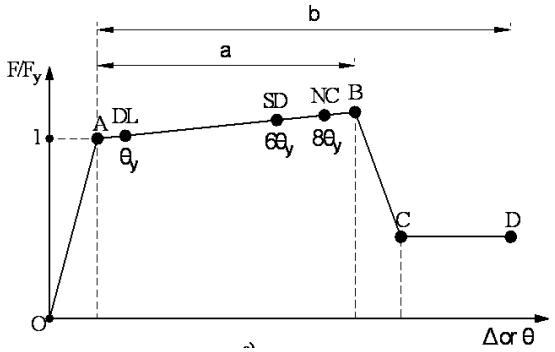

Figure 2. Performance curve as per FEMA356 [3].

Right next to point A, the limit DL - damage limitation is given, which corresponds to the occurrence of yielding in the beam element. The line AB depends on the material characteristics of the element and usually represents 10% of the slope of the line OA [3]. The point SD - corresponds to Significant Damage to the elements and is quantified by $6\theta_y$. The point NC-Near Collapse, represents a state close to failure of the element and it, according to Table 6.25, FEMA 356 [3], is quantified as: $8\theta_y$. It is evident that the value of the q-factor also depends on the plastic capacity of rotation of the elements. According to Eurocode 8, the criteria for the plastic rotation

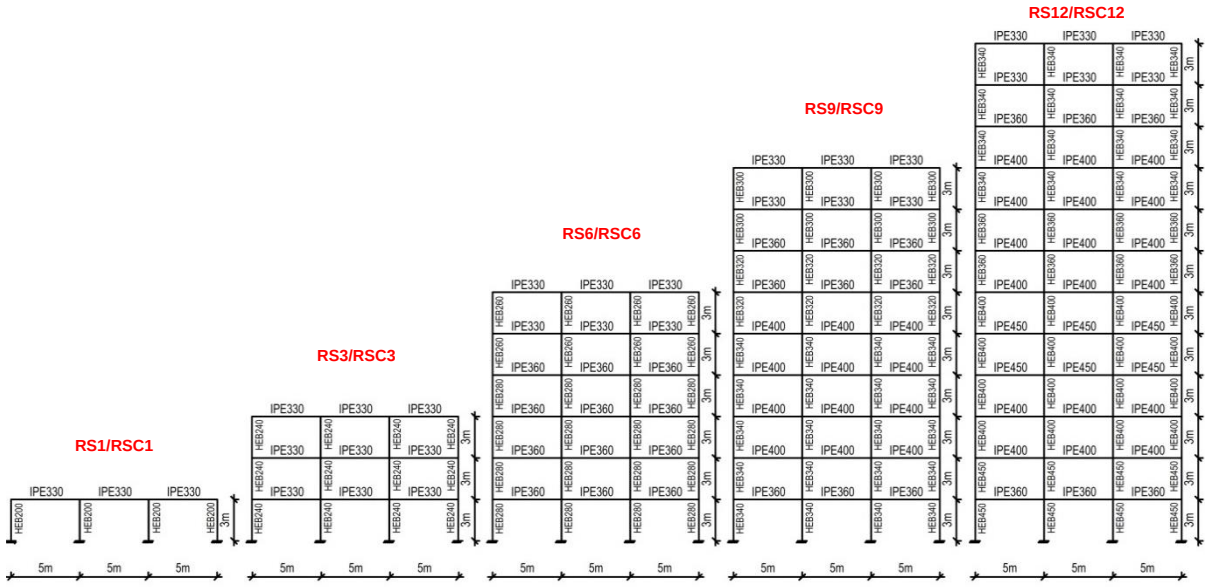

Figure 3. The studied frames.

capacity of the elements, which can define the ultimate capacity of the system, are not explicitly mentioned.

The ultimate capacity of rotation of the columns of the ground floor corresponding to the NC state, i.e. the maximum plastic rotation with a value of $8\theta_y$, has been chosen as the limit performance for the frames of this paper. In the following, the procedure according to the provisions of FEMA356 is given to determine the rotation capacity for beams and columns, respectively. M_p–the plastic moment of the element, L_b– the length of the beam, L_c –the length of the column, I_b –the moment of inertia of the beam, I_c–the moment of inertia of the column, N–the axial force in the columns (from the seismic combination) and N_p - the plastic axial bearing capacity of the column, the corresponding parameters from relations (5) and (6) are indicated. The rotation during plasticization of the beam and column, is given by the following expressions [3]:

$$\theta_{b,y} = \frac{M_p L_p}{6EI_b};\ \theta_{c,y} = \frac{M_p L_c}{6EI_c}\left(1 - \frac{N}{N_p}\right) \qquad (1)$$

In the second group, the same frame configurations are analyzed as composite frames and they are labeled as RSC1, RSC3, RSC6, RSC9 and RSC12. A composite slab d_c = 120 mm and an effective width of 1 m was chosen. In Figure 3, the analyzed frames are shown. The constant load varies from 27-45kN/m', while the variable load has a constant value of 11 kN/m'.

2.2 MODELING OF ELEMENTS

The nonlinear characteristics of the sections are modeled with the Distributed Plasticity approach. Distributed plasticity (Distributed Plasticity), compared to the Concentrated Plasticity (Lumped Plasticity), allows the distribution of plasticity along the entire length of the element and is not limited by the calibration of the parameters depending on the examined element, [6]. It is assumed that full interaction is provided between the section elements in the concrete and steel section.

3. STUDIED FRAMES

The subject of this paper's analysis are two groups of moment frames. In the first group, a series of steel moment frames with 1, 3, 6, 9, and 12 levels are analyzed and labeled as RS1, RS3, RS6, RS9, and RS12, respectively. The analysis was carried out with an assumed PGA=0.35g, damping coefficient ξ=5%, soil category B, Type 1 of the response and assumed value of the behavior factor q=4.

The advantage of this formulation comes into consideration especially when it is necessary to model the elements with variable stiffness along the length, such as the composite beams [5], [12]. Namely, with the distributed plasticity, the integration of the non-linear geometric and material behavior is carried out at the cross-sectional level. The cross-section is discretized into a series of infinitesimal cross-sections, called fiber-sections. At the same time, an axial dependence between stresses and dilations is

established on each of these fiber-sections. That is, for each of the fiber sections, the normal stress is determined individually.

The longitudinal element is discretized into a finite number of Gaussian points. To obtain the influences along the length of the element, the Gaussian points are integrated. In this way, along the length of the section, the possible positions of the formation of the plastic hinges are controlled. The number of fiber - elements for the composite frame is 200. It is assumed S235, Strain - hardening 0.005 and E_s = 210 000 N/mm^2. While for concrete: f_{ck}= 30 N/mm^2, f_{ct} = 0.001 N/mm^2, crushing strain $\epsilon_c = 0.0022$ and E_c = 32836 N/mm^2. For this method to give solid results, the element should be divided along its length. Within this paper, a division of each of the elements into 6 equal parts has been made. Each of those 6 elements, is divided into 10 points for Gaussian integration

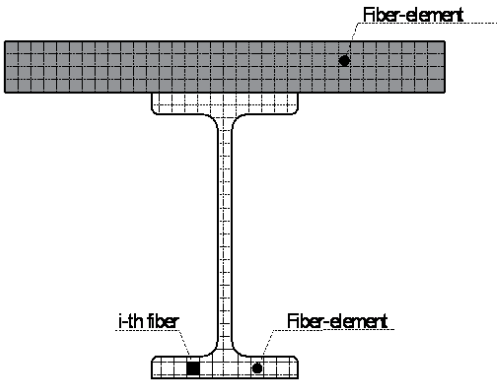

Figure 4. Discretization of the composite cross-section with “fiber” elements

4. ANALYSIS OF OBTAINED RESULTS

In this paragraph follows the presentation and discussion of the obtained results. In each of the graphs shown in Figure 5 the Pushover curves obtained from the nonlinear static analysis for determining the q-factor are shown.

In Figure 5a) it is observed that ultimate displacement corresponding to the performance limit PL (Performance Limit) ($8\theta_y=\theta_p$), is almost identical for RS1 and RSC1, respectively. The differences are evident in the displacements at the formation of the first plastic hinge, that is, the ductility factor for RS1 is 56% higher than RSC1(Figure 5a and 6c).

By increasing the number of levels, an increase of the overstrength factor ($\alpha = \mathrm{R}_\Omega \cdot \mathrm{R}_\rho$) is observed for both frames (RS3 and RSC3, 1.355 and 1.302, respectively (Figure 5b and 6c). Also, the ultimate horizontal force and the occurrence of the first plastic hinge, for RSC3 are 21.3% and 26% higher compared to the values obtained for RS3 (Figure 6c). On the other hand, the ductility factor of RS3 is 53% higher in comparison with RSC3 (Figure 6d). And in this case, the q-factor for the pure steel frame is 23% higher compared to the composite frame (Figure 6a). From Figure 6c) there is a drop again in the factor for the of RS6, with a total value of 1.17. The large value of the N/Np ratio can be considered as the reason for this decline. On the other hand, for RSC6, at the same value of N/Np, this factor is α_{sc}=1.24 (Figure 6c). There is also a decrease in ductility factor for the RS6 frame, which is 3.33 (Figure 6d). In the case of the composite frame (RSC6), there are no visible decreases in μ_{cs}. Namely, in this case, the q-factor for the steel frame is higher compared to the composite frame (Figure 6a).

From Figure 6d), a drop in the α_{sc} –factor for the of the steel frame is observed, which is α_s=1.109. This is due to the large value of the N/N_p ratio, while in the composite frame, we have a visible increase in α_{sc} compared to RSC6, and a 25% increase compared to RS9. A decrease is also observed in the ductility factor of RS9, while in the case of RSC9, we have an unchanged value (Figure 6d). In this case, the q-factor of the steel frame is lower compared to the composite frame (Figure 6a). In the last group frames (RS12&RSC12), again the α –factor of the steel frame is lower in comparison to the composite frame, by 13.5% (Figure 6c). It is observed that the ductility factor for the steel frame has a value (μ_s=2.62) similar to that of the composite frame (μ_{cs}=2.74). As an implication of this, for RS12, the q-factor is 3.9 and it is also lower compared to RSC12. In the following, the course of changing several of the dynamic characteristics of the considered frames is given, by increasing the number of levels and, accordingly, by varying their stiffness characteristics.

From Figure 6a), the reduction of the q-factor can be clearly seen for both the steel and the composite frames, with an increase in the number of levels. From level 6 to level 12, the q-factor for both frame categories has similar values. The differences are more evident for lower heights.

On the other hand, from Figure 6 b), it is clearly seen that for the first group of frames (RS1 and RSC1), the relative floor displacements are

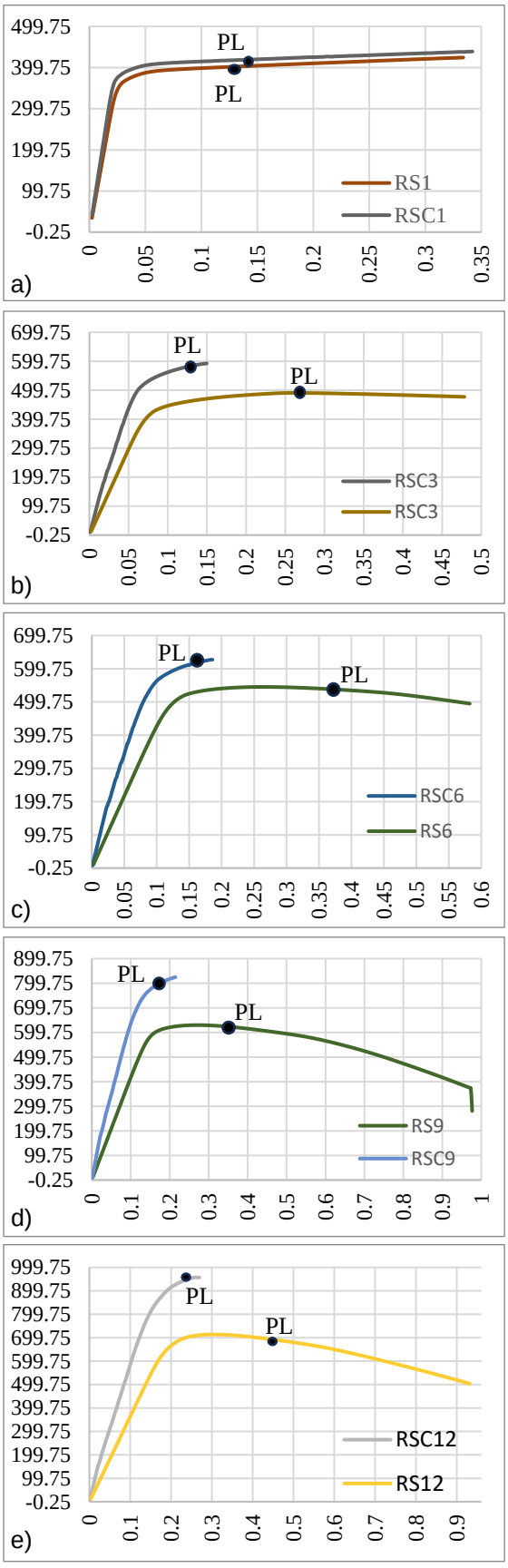

Figure 5. Comparison of Pushover curves for: a) RS1&RSC1; b) RS3&RSC3; c) RS6&RSC6; d) RS9&RSC9; e) RS12&RSC12.

almost identical. With the increase in the number of levels, in the composite frames, there is a gradual decrease in the relative storey displacements, by 18.1%, 32.2%, 43.7% and 31.2% for RSC3, RSC6, RSC9 and RSC12 (relative to RS3, RS6, RS9 and RS12), respectively.

Figure 6c), shows the overall global change in the overstrength factor for both group of frames. Except for RS3, all considered steel frames have a value of 1.17 for this parameter. Although these frames belong to the group of multi-storey and multi-bay frames, if the performance limit is defined in advance (as in this example with ultimate rotation capacity of the ground floor columns) obtained values for overstrength (α) factor would be less than 1.3.

On the other hand, for the composite frames, except for RSC1 (where α_{sc} =1.12), the values for α_{sc} gradually increase and they can be considered to be in the margins of the recommended value according to Eurocode 8, i.e. 1.3, although for them the ratio N/Np>0.25.

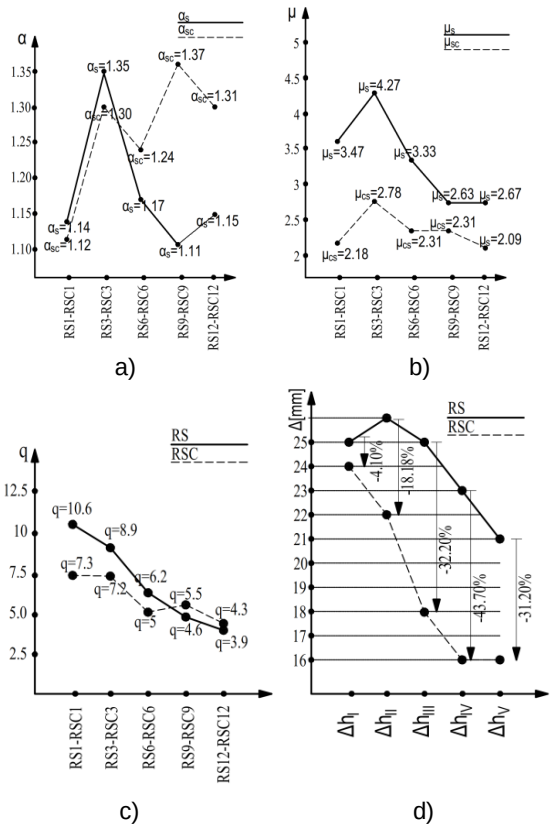

Figure 6. Graphical representation for the considered group of frames: a) behaviour factor, b) relative storey displacements, c) overstrength factor, d) ductility factor

The change in ductility factor for both frame categories is shown in Figure 6 d). In the case of steel frames, for storey 1 and storey 3, these

values are relatively large (3.43 and 4.27, respectively). With increasing levels, a gradual decrease in this parameter is observed for steel frames. On the other hand, the situation with composite frames is different. Namely, there is a more constant distribution of the ductility factor and the same, regardless of the height change, ranges from 2 to 2.78.

4. CONCLUSION

In this paper, a sensitivity analysis is carried out for the two categories of moment frames, dimensioned according to the rules provided in EC3 and in EC8. The parameters that make up the q-factor are determined for both the composite and the steel frames. The influence of the effects of the composite beams, the number of frame levels, the stiffness characteristics ("Strong Columns/Weak Beams" criterion), the local behavior of the ground floor columns and the limit performance of the structures are taken into account, all in order to see the change of the behavior factor. In doing so, the following conclusions were drawn:

Composite beams have an influence on the increase of the design reserve capacity (R_Ω) and redundancy factor. (R_ρ) (up to 23%) in the composite frames compared to the pure steel frames. It is also observed that these parameters increase with an increase in the number of levels in composite frames (Figure 6, c));

Due to the fact that the frames were dimensioned by the dominant action of permanent loads, it is observed that although the ratio (N/Np)≤0.25 is not fulfilled for RSC6, RSC9 and for RSC12, still reserve capacity (R_Ω) and redundancy factor for the composite frames, is in the boundaries proposed by EC8. On the other hand, with steel frames, except for RS3 (where the criterion N/Np=0.232 is met), for all higher levels, lower value for $\alpha = R_\rho \cdot R_\Omega$ than 1.3 is obtained.

The ductility factor (R_μ) for steel frames is relatively high for RS1 and RS3, while with increasing levels, this parameter tends to decrease. In the case of composite frames, R_μ shows more even changes (Figure 6, c));

At composite frames, a reduction in horizontal relative storey displacements was also observed compared to the steel frames. For RSC6, RSC9 and RSC12, this reduction amounts to over 30%, compared to steel frames with the same number of levels.

REFERENCES

[1] ATC-34. ,,A Critical Review of Currnet Approaches to Earthquake- resistant Design". Applied Technology Council, Redwood City, California, 1995.

[2] Denavit. M et al.: ,,Seismic performance factors for moment frames with steel- concrete compoiste columns and steel beam". Earthquake engineering&structural dynamics. Wiley Online Library. DOI: 10.1002/eqe.2737.

[3] FEMA 356: ,,Prestandard and Commentary for Seismic Rehabilitation of Buildings". American Society of Civil Engineers for the Federal Emergency Management Agency, Washington. 2000.

[4] Ferraioli. M, Lavino. A, Mandara. A : ,,Behaviour Factor of Code-Designed Steel Moment-Resisting Frames". International Jurnal of Steel Structures, 14(2), pp. 243-254, 2014.

[5] Gharakhanloo. A: ,,Distributed and concentrated inelasticity beam-column elements used in earthquake engineering". Master Thesis, Civil and Environmental Engineering, NTNU-Tronheim, June 2014 .

[6] Huu. C, Kim. S: ,,Practical nonlinear analysis of steel-concrete composite frames using fiber-hinge method". Jurnal of Constructional Steel Research, 74 (2012) 90-97, ELSEVIER.

[7] Landolfo. R et al. :,,Design of steel structures for building in seismic areas". Eurocode 8- Design of structures for earthquake resistance. Part 1-1- general rules, seismic actions and rules for buildings. ECCS. Wiley, 2016.

[8] Martinez. R, Elnashai. A: ,,Confined concrete model under cyclic load". Mater. Struct. 30: 139-147. 1997.

[9] Mazzolani. F, Piluso. V: ,,Theory and design of seismic resistanat steel frames". Spon Press. Tylor & Francis Group, 1997.

[10] Yahmi.D,Branci. T, Bouchair. A and Fournely. E,: ,,Evaluating the Behaviour Factor of Medium Ductile SMRF Structures". PeriodicaPolytechnica, Civil Engineering. 62(2), pp. 375-385,2018.

[11] ASCE: ,,Minimum Design Loads for Buildings and Other Structures". American Society of Civil Engineers, New York. 2010.

[12] Mander. J, Priestly. M: ,,Theoretical stress-strain model for confined concrete". J. Struct. Eng.114.1804-1826. 1988.

[13] Eurocode 3: Design of steel structures - Part 1-1: General rules and rules for buildings.

[14] Eurocode 8: Design of Structures for Earthquake Resistance- Part 1: General rules, and rules for buildings.

Artur Roshi
PhD
Metropolitan University of Tirana
Albania
artur.roshi@yahoo.com

Golubka Nechevska - Cvetanovska
PhD, Emeritus Professor
Ss. Cyril and Methodius University in Skopje
Institute for Earthquake Engineering and Engineering Seismology
N. Macedonia

Jordan Bojadjiev
PhD, Assistant Professor
International Balkan University, Skopje
N. Macedonia

EXPERIMENTAL TESTS AND ANALYTICAL INVESTIGATION OF RC BUILDING COLUMNS STRENGTHENED BY CFRP

The need for repair and strengthening of RC buildings and their structural elements occurs when their elements do not possess sufficient strength, stiffness and/or ductility out of different reasons or due to slighter or more severe damages most frequently caused by earthquakes. Within the frames of this paper, special emphasis will be put on RC buildings where, during construction, the built-in concrete has not achieved the designed concrete class and/or buildings that cannot satisfy the required strength, stiffness and deformation characteristics particularly in earthquake conditions due to built additional storeys or enlargements. In these cases, it is necessary to take measures for repair and strengthening using traditional or Innovative Materials. In this paper, focus will be given on technology of strengthening of RC columns with innovative materials as well as characteristics and types of these material will be introduced.

To present the possibilities and the benefits of use of these innovative construction materials in strengthening of structural elements of buildings and integral building structures, ample laboratory research for definition of the characteristics of these materials with different technologies of strengthening by CFRP (Carbon Fiber Reinforced Polymers) materials are carried out at the Institute of earthquake Engineering and Engineering Seismology – IZIIS, Skopje. Selected results of experimental and analytical investigations of RC column models with different technologies of strengthening by CFRP are presented.

Keywords: quasi-static tests, innovative materials, CFRP, repair and strengthening, strength, ductility

1. INTRODUCTION

Behaviour of structures constructed and built of reinforced concrete during their serviceability period as well as during earthquakes depends

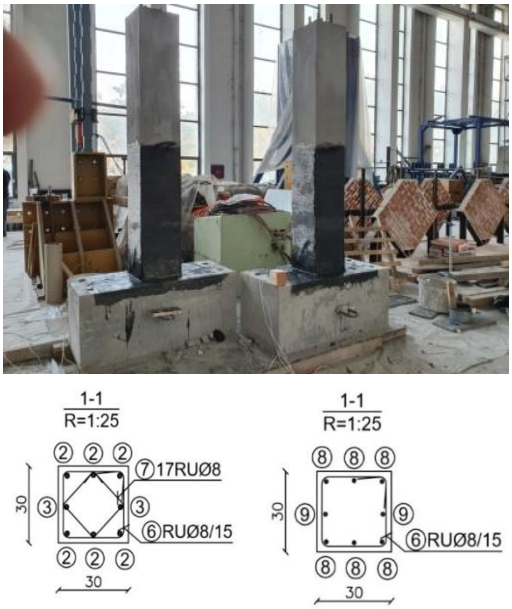

Figure 1. Construction of the column models (Model M1 and Model M2) for experimental tests.

on many factors. On one hand, there are the external factors, i.e., loads acting upon the structures (in addition to the main loads, there are also additional loads as well as effects caused by possible explosions, fires, earthquakes), while on the other hand, there are the factors that directly depend on the very structure of the buildings (structural system, type, quality and quantity of material used for the construction of the structure, the number of storeys, the mode of foundation etc.). All these factors directly affect the strength and deformation characteristics of the individual structural elements and the structural system as a whole.

It has been a usual practice to perform repair and strengthening of structures by application of traditional methods (most frequently, jacketing of elements), but lately, new innovative materials with a special technology of construction and repair have increasingly been applied. The application of these materials is still the subject of a large number of investigations worldwide, particularly in the field of application of these materials in seismically active regions.

In this paper, there are some parts of the results from quasi-static experimental investigation of two RC column models and some part of analytical investigation for Definition of Real Strength and Deformability Capacity of Column Models strengthening with CFRP.

Figure 2a. Construction of the column models for experimental tests

Figure 2b. Construction of the column models for experimental tests and instrumentation

2. EXPERIMENTAL PROGRAM FOR QUASI-STATIC TESTS PERFORMED AT UKIM-IZIIS

For the needs of own experimental investigations, two column elements were designed. The column models were designed as fixed cantilever girders with a constant length of both models of 200 cm (the column was treated only up to the inflection point, i.e., half of the total height) and cross-section of 30/30 cm. In both models, the varying parameters were, the percentage of longitudinal and transverse reinforcement and the axial forces. The concrete class, i.e., the compressive strength of concrete and the type of the CFRP was same for both models. The elements were designed to the geometrical scale of 1:1(Figure 1) [10].

Model M1 has 8∅18 as longitudinal reinforcement and stirrups ∅8 at a distance of 15/7.5 cm. and Model 2 has 8∅14 as

Figure 3. Test set-up

longitudinal reinforcement and stirrups ∅8 at a distance of 15 cm.

Photos taken during construction of the models (Model M1 and Model M2), are presented in Figure 1, Figure 2a and Figure 2b., Photos and results obtained in the process of quasi-static tests on Model M1 and Model M2 (Figure 3) are presented further.

The models were instrumented with 6 strain gages, out of which 2 were placed outside on the concrete and 4 were on the longitudinal reinforcement, placed and protected before concreting of models.

For performing the tests, quasi-static equipment available in the Laboratory for dynamic testing in IZIIS, was set in appropriate position [1].

Before starting with application of the alternative horizontal force (LC 1), axial force of 500 kN was applied in the column – Model 1, i.e. axial force of 300 kN in the column – Model 2, simulating the gravity load (LC 2).

The process was controlled by the displacement, in several repeated cycles, up to reaching heavy damage of the models.

The testing was performed by application of increasing displacement steps up to failure of the models.

The following sections contain the processed results from the quasi-static tests of model M1 and model M2 along with conclusions.

2.1. RESULTS OF MODEL M1

During the tests, a vertical force of 500 kN was first applied on the column (LC2 (Figure 4). During application of the horizontal force (LC1), the values of strain (in both concrete and reinforcement) as well as the displacements at the point of application of the horizontal force (LVDT) were measured. Channels SG_1 and

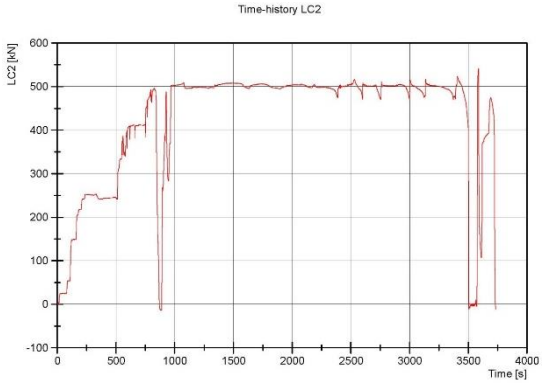

Figure 4. Time histories of applied vertical force LC2 and strains (SG) during the test of Model M1.

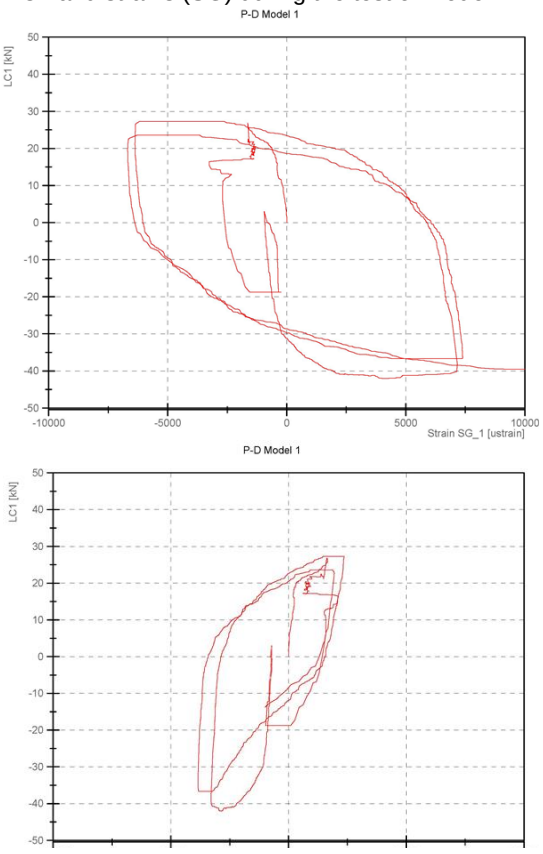

Figure 5. Force LC1 – strain relationship (SG_1) and (SG_3) for Model M1 .

SG_2 measured the strains in the concrete, while SG_3, SG-4, SG-5 I SG_6 measured strains in reinforcement in both directions (Figure 5).

Based on the data obtained, hysteretic curves LC1 were obtained with SG_1, and SG-3 presented in Figure 5, it can be concluded that the model exhibits an excellent hysteretic behaviour. This points to the fact that Model M1 in this period has a high capacity for energy absorption, i.e., it exhibits a good hysteretic behavior with obtained high capacity for displacement.

For a value of ε_s = 1.94 ‰ in steel (the yielding point of reinforcement), displacement of 10.065 mm and force of 38.39 KN were achieved.

The maximum measured displacement at the free end of the model M1 in positive direction was 55.3 mm, while during the last test, the displacement was already very high. The maximum achieved horizontal force was 47.5 KN.

2.2. RESULTS OF MODEL M2

During the tests, vertical force of 300 kN was first applied upon the column (LC2). During the application of horizontal force (LC1), the values of strains (epsilon in both concrete and reinforcement) as well as displacements at the point of application of force were measured (LVDT). At channels SG_1 and SG_2, strains in concrete were measured, while at SG_3, SG-4, SG-5 I SG_6, strains in reinforcement were measured in both directions (Figure 6, Figure 7 and Figure 8).

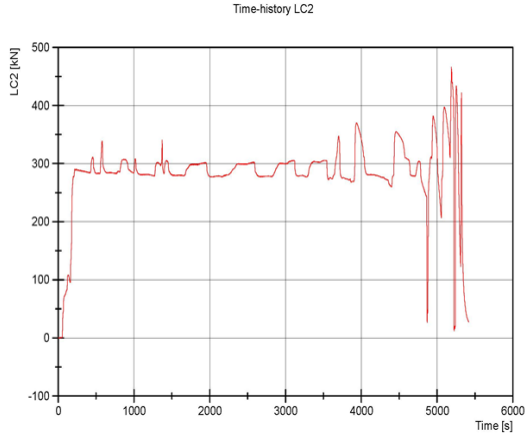

Figure 6. Time histories of applied vertical force LC2 during the test for Model M2

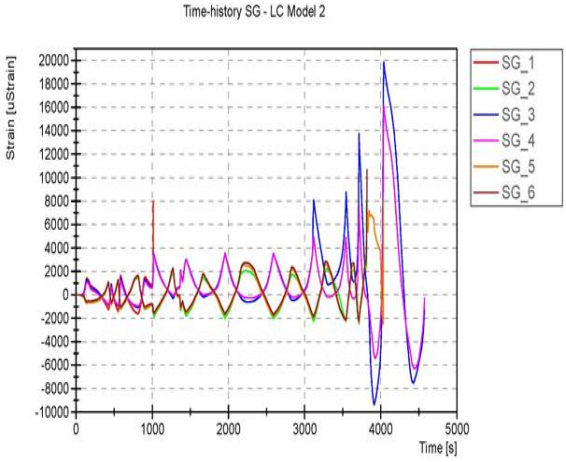

Figure 7. Time histories of strains (SG), during the test, Model M2, up to 5000 points.

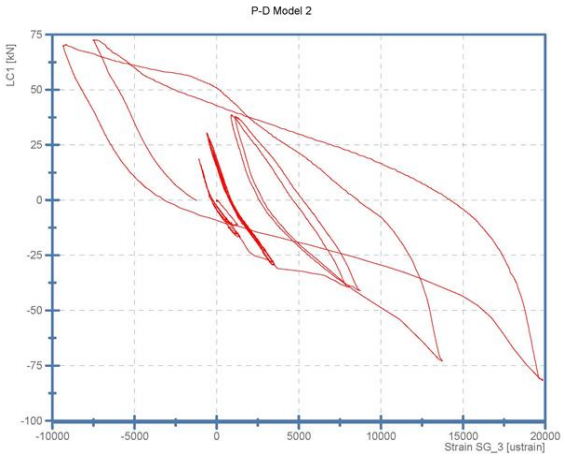

Figure 8. Relationship force – SG_3 for model M2

Based on the data obtained, the best hysteretic behavior, with regular hysteretic curves, was obtained at SG_3 and SG_4, which points to the fact that this model also exhibits hysteretic behavior, but with a lower capacity for energy absorption compared to Model M1.

The maximum measured displacement at the free end of the model M2 in positive direction was 69.28 mm. The maximum achieved horizontal force was 68.5 KN.

The observed damages during the quasi-static testing of Model M1 are presented in Figure 9.

Figure 9. Observed damages during the quasi-static testing of Model M1

Figure 10. Observed damages during the quasi-static testing of Model M2.

The observed damages during the quasi-static testing of Model M2 are presented in Figure 10.

The following comments can be mentioned regarding the models' behavior during the testing:

- The failure of the CFRP was sudden followed by specific sound and by crashing of concrete.
- The concrete quality was not good enough and it was easy to remove the particles after cutting of the CFRP.
- There was visible bending of the longitudinal reinforcement after test accomplishment.

3. DEFINITION OF REAL STRENGTH AND DEFORMABILITY CAPACITY OF COLUMN MODELS

To define the real bearing and deformability capacity of the built column models, the values on quality of built-in concrete and reinforcement obtained for both vertical and transverse reinforcement, as well as the type of used CFRP were used. In the first phase, the real M-Φ (moment – curvature) relationships of the column cross-sections were computed by applying axial force, the real M-N diagrams, and then, based on the obtained M-Φ diagrams, the

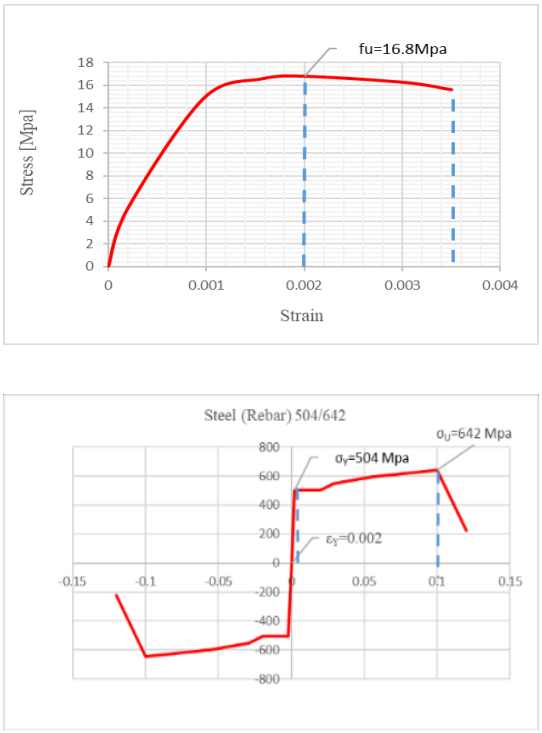

Figure 11. Stress-strain relation for non-linear structural analysis for concrete C16/20 and for rebar RA 504/642

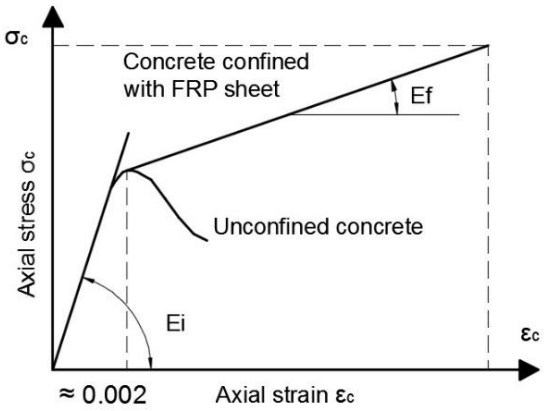

Figure 12. Ideal axial stress-strain diagram σc-εc for concrete confined with a CFRP sheet

strength and deformability capacity of each model was defined.

The strength and deformability characteristics (M-N) and (M-Φ) at cross-section level were analytically defined by use of the SAP2000 computer software. The following analyses were carried out:

For Model M1, definition of the M-Φ diagram for Nv = 500 kN and M-N diagram (Figure 13) for the following values for 0.1, 0.2, 0.3 series:

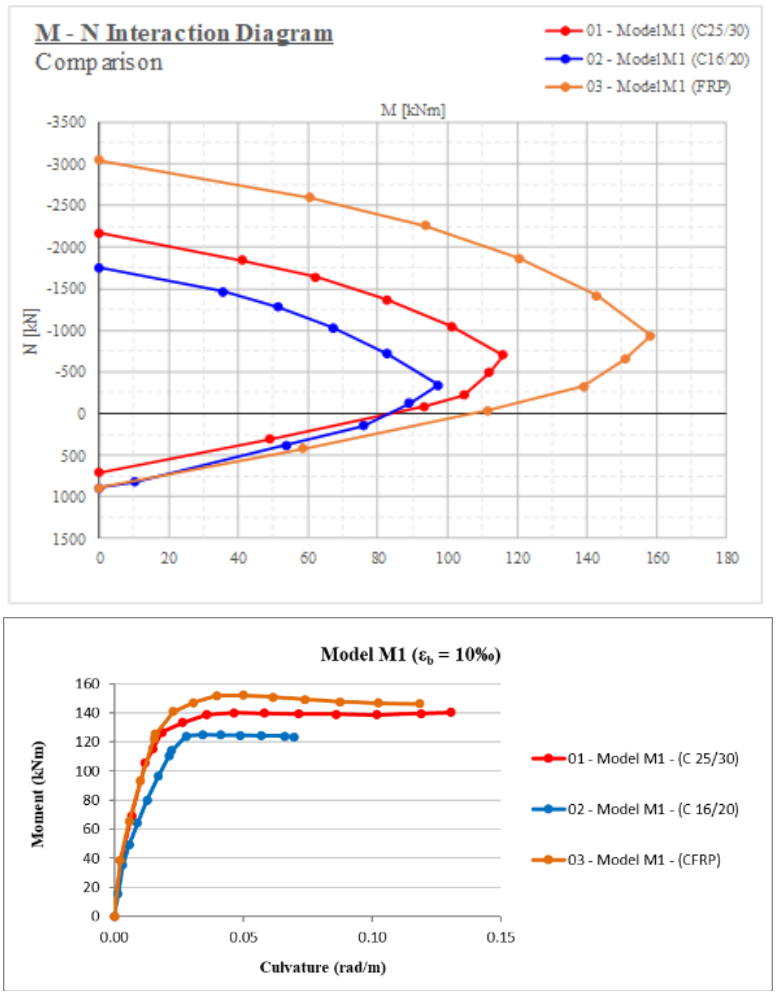

Figure 13. M-N and M-Φ Diagrams for Model M1 - Comparison

- For the designed concrete class (DC) (EC-25/30) with quality and quantity of reinforcement.
- For the built-in concrete class (CC) (EC-16/20) with quantity and quality of reinforcement.
- For the built-in concrete class with one layer of CFRP (CC-FRP) (38/46) with quantity and quality of reinforcement.

For Model M2, definition of the M-Φ diagram for Nv = 300 kN and M-N diagram (Figure 14) for the following values for 0.1, 0.2, 0.3 series:

- For the designed concrete class (DC) (EC-25/30) with quality and quantity of reinforcement.
- For the built-in concrete class (CC) (EC-16/20) with quantity and quality of reinforcement.
- For the built-in concrete class with one layer of CFRP (CC-FRP) (38/46) with quantity and quality of reinforcement.
- For all analyses of RC cross-sections without CFRP, the working diagrams (σ-ε) for concrete and the working diagram of steel shown in Figure 11 were used. All analyses were done by taking into consideration confinement of the cross-section of transverse reinforcement.

For the concrete wrapped with CFRP, the working diagram shown in Figure 12 was used [3].

The results obtained from these analyses are presented in the following sections.

3.1 M-N AND M-Φ RELATIONSHIP FOR MODEL M1

Presented for Model M1 are the results from three series of analyses (0.1, 0.2, 0.3 series) performed for definition of M-N and three series for M-Φ diagrams. All of the presented diagrams have been obtained by use of the SAP2000 program. The M-N interaction diagrams are displayed in Figure 13, which clearly shows the difference among all three series of analyses.

The M-N and M-Φ comparative diagrams for Model M1 are presented in Figure 13.

3.2 M-N AND M-Φ RELATIONSHIP FOR MODEL M2

Presented for model M2 are the results from three series of analyses (0.1, 0.2, 0.3 series) for definition of M-N and M-Φ diagrams (Figure 14). All of the presented diagrams have been obtained by use of the SAP2000 program. The interaction diagrams clearly show the difference among the all series of analyses. The moment capacity for the 03 series (cross-section with CFRP) is higher than that of cross-section 02 (series with built-in concrete class of 16/20) for 63%. The capacity of axial forces for the 03 series (cross-section with CFRP) is higher in respect to that of cross-section 02 (series with built-in concrete class of 16/20) for 59.5%.

The M-N and M-Φ comparative diagrams for Model M2 are presented in Figure 14.

Based on the analyses of the results from Table 1, it can be concluded that the ductility to rotation for Model M1 is 2.049 greater for the model with CFRP, while the ductility to displacement is greater in respect to the ductility of Model M1 without CFRP for 76.7%.

In the case of Model M2, the ductility to rotation is higher in the case of the Model with CFRP for 64 %, while the ductility to displacements is higher compared to the ductility of the Model M2 without CFRP for 46.1%.

4. CONCLUSION

The following analyses were carried out: The moment capacity obtained for cross-section of Model M1 with CFRP is greater for 21.07 % than that of cross-section without CFRP and the ductility to rotation is higher in the case of the model with CFRP for 98 %. The moment

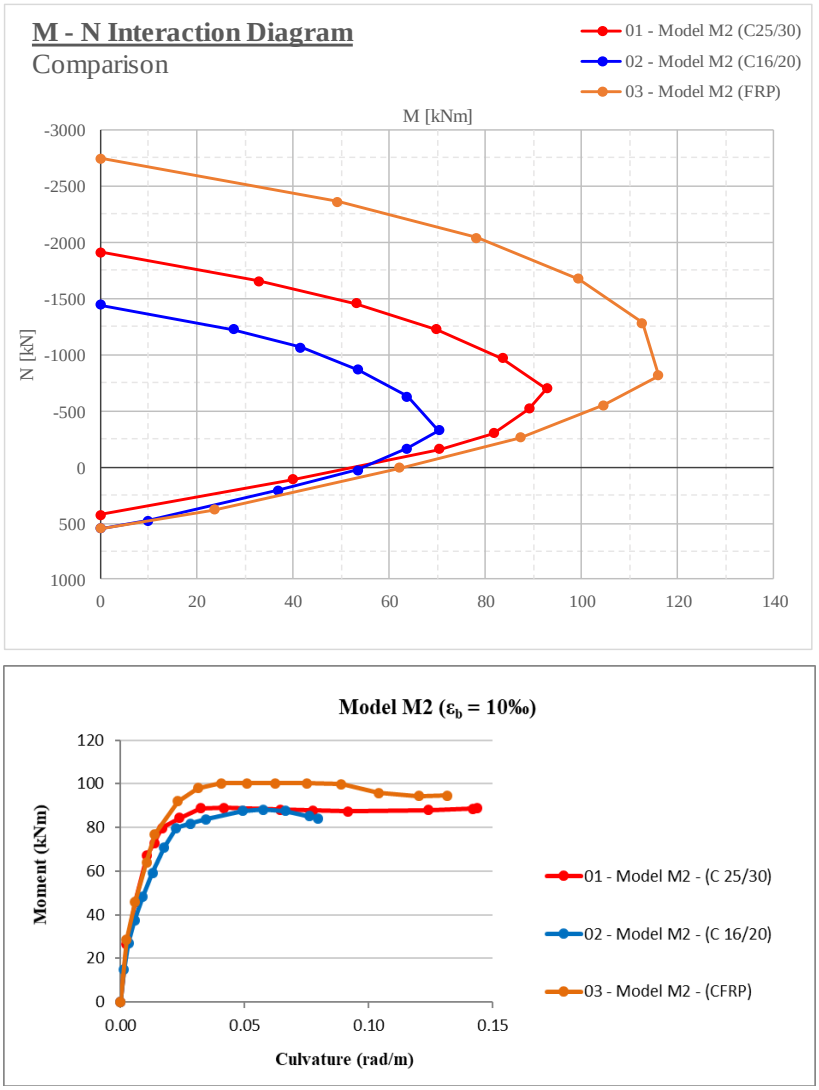

Figure 14. M-N and M-Φ Interaction Diagrams for Model M2 - Comparison

Table 1. Rotation and displacement capacity for Model M1 and Model M2

Specimen	Rotation		Displacement		Ductility
	Φy [rad/m]	Φu [rad/m]	dy [cm]	du [cm]	Dd
Model M1-02	0.0127	0.0696	1.056	2.626	2.487
Model M1-03	0.0154	0.1730	1.281	5.631	4.306
Model M2-02	0.0128	0.0663	1.065	2.542	2.387
Model M2-03	0.0231	0.1963	1.922	6.702	3.487

capacity obtained for cross-section of Model M2 with CFRP is greater for 7.7 % than that of cross-section without CFRP and the ductility to rotation is higher in the case of the model with CFRP for 64 %.

Sample analytical analyses were carried out to define the strength and deformability capacity (M-N) and (M-Φ) at cross-section level were analytically defined by use of the SAP2000 computer program. Based on the obtained M-Φ diagrams, the strength and ductility capacity of each model was defined. The rotation and ductility capacity for model M1 and model M2 are greater than the models without CFRP.

Generally, it can be concluded that FRP systems represent a very practical tool for strengthening and retrofitting of concrete structures and are appropriate for flexural strengthening, shear strengthening and column confinement and ductility improvement.

REFERENCES

[1] Krstevska, L., Nechevska- Cvetanovska, G. (2019), Quasi-static testing of column models strengthened by FRP, UKIM-IZIIS, IZIIS Report 2019-75.

[2] CNR-DT 200/2004. Guide for the Design and Construction of Externally Bonded FRP Systems for Strengthening, 2004 (Downloaded free from: http://www.cnr.it/sitocnr/IlCNR/Attivita/NormazioneeCertificazione/NormazioneeCertificazionefile/IstruzioniCNR DT200 2004 eng.pdf).

[3] M. DI Ludovico, A. Prora, G.Manfredi and E.Gosenza, “Seismic Strengthening of an Under-design RC Structure with FRP”, Department of Structural Engineering, University of Naples Federico II, Naples, Italy, Published online 24 August 2007 in Wiley InterScience.

[4] G. Necevska - Cvetanovska and R. Petrushevska (2000). “Methodology for Seismic Design of R/C Building Structures“. 12WCEE, New Zeland.

[5] Necevska - Cvetanovska, G., Apostolska, R. (2012). Methodology for Seismic Assessment and Retrofitting of RC Building Structures, Proc. of 15 World Conference on Earthquake Engineering (Paper ID 2149), 24-28 September 2012, Lisbon, Portugal.

[6] Necevska – Cvetanovska, G., Roshi, A. “Rehabilitation of RC Buildings in Seismically Active Regions Using Traditional and Innovative Materials”, Journal Building Materials and Structures, Novi Sad, Serbia, 62 (2019) 3 (19-30).

[7] Nechevska-Cvetanovska, G., & Roshi, A. (2019). Rehabilitation of RC buildings in seismically active regions using traditional and innovative materials. Građevinski materijali i konstrukcije, 62(3), 19-30.

[8] Nechevska-Cvetanovska, G., Roshi, A., & Bojadjieva, J. (2019). Seismic strengthening of existing rc buildings structures using concrete jacketing and frp materials. E-GFOS, 10(19), 68-80.

[9] Roshi, A., Nechevska- Cvetanovska, G. (2019). Repair and Strengthening of RC Buildings using Traditional and Innovative Materials, 18th International Symposium organized by Macedonian Association of Structural Engineers (MASE), October 4-7, 2019, Ohrid, Macedonia.

[10] Roshi, A., (2020). Application of innovative buildings materials for repair and strengthening of RC columns in seismically active regions, Doctoral dissertations, Ukim Iziis Skopje, Macedonia.

Zlatko Srbinoski
PhD, Full Professor
Ss. Cyril and Methodius University in Skopje
Faculty of Civil Engineering
N. Macedonia
srbinoski@gf.ukim.edu.mk

Zlatko Bogdanovski
PhD, Associate Professor
Ss. Cyril and Methodius University in Skopje
Faculty of Civil Engineering
N. Macedonia

Filip Kasapovski
PhD, Assistant Professor
Ss. Cyril and Methodius University in Skopje
Faculty of Civil Engineering
N. Macedonia

Tome Gegovski
MSc, Teaching Assistant
Ss. Cyril and Methodius University in Skopje
Faculty of Civil Engineering
N. Macedonia

Filip Petrovski
MSc, Teaching Assistant
Ss. Cyril and Methodius University in Skopje
Faculty of Civil Engineering
N. Macedonia

CRITERIA AND STANDARDS FOR SELECTING A NEW STATE CARTOGRAPHIC PROJECTION

The selection of a new State cartographic projection is a fundamental cartographic activity at the state level, upon which the quality of spatial data will rely for an extended duration.

The paper shows the basic criteria for the selection of a new State cartographic projection, as well as the evaluation of the proposed projections for the selection of a new State cartographic projection of the Republic of Macedonia.

Keywords: states cartographic projection, Transverse Mercator projection

1. INTRODUCTION

The State cartographic projection is a fundamental cartographic standard, which defines the processing and visualization of spatial data at the national level. All geodetic activities aimed at the acquisition of spatial data, as well as standardized cartographic products, must comply with the standards imposed by the State Cartographic Projection and the State Coordinate System.

When it comes to the Republic of Macedonia, the activities for the selection of a new State cartographic projection began 25 years ago. Those activities are generally the result of the works (scientific topics, doctoral dissertations [3], etc.) of the members of the Chair of Advanced Geodesy at the Faculty of Civil Engineering in Skopje.

The series of papers ([4], [5], [6], [7], [9]), that have been published in the Scientific Journal of Civil Engineering in the past period, which treat the characteristics and the possibility of applying a series of conformal cartographic projections on the territory of the Republic of Macedonia, are in that direction.

Thus, this paper summarizes part of the analyzes and conclusions related to the criteria and standards used in the selection of the new State cartographic projection of the Republic of Macedonia.

2. CRITERIA FOR THE SELECTION OF A NEW STATE CARTOGRAPHIC PROJECTION

The criteria for assessing the quality of projections aim to achieve a comprehensive and optimal selection of the new State cartographic projection.

The analysis of cartographic projections based on the specified criteria should lead to the selection of a national cartographic projection that incorporates recommendations and experiences from international bodies in the field of geodesy and cartography. This selection process should also prioritize the national interests of the Republic of Macedonia in defining the National Spatial Reference System. Some of the mentioned criteria are quantitative, while others are qualitative, introducing additional aspects for evaluating the quality of the projections.

The primary mathematical (quantitative) criteria include:

- Size (maximum and average values) of linear deformations.
- Size of surface deformations.
- Maximum value of meridian convergence.
- On the other hand, qualitative criteria for evaluating projections encompass:
- Regularity in the distribution of linear and surface deformations, expressed through the arrangement of respective isolines.
- Simplicity and completeness of the mathematical model.
- Economic aspects of implementing the new projection.
- Tradition.
- Adherence to contemporary European standards in the field of state cartographic projections.

Research for the selection of a new State cartographic projection begins with the examination of factors influencing the choice and the criteria used to evaluate the proposed projections. As a fundamental factor influencing projection selection, the mathematical-geographical position of the national territory is highlighted, encompassing:

- Spatial distribution,
- Dimensions, and
- Shape of the national territory.

The spatial arrangement of the Republic of Macedonia is defined by its location in the northern hemisphere at around the 42nd parallel and the meridian with a geographical longitude of $\lambda = 22°$. The surface area of the national territory is 25,713 km², with a total length of the border line being 889 km. The maximum distance between two points along the national border is 216.1 km, and the radius of the circle described using the distance between border points and the central point of the national territory is 115.1 km.

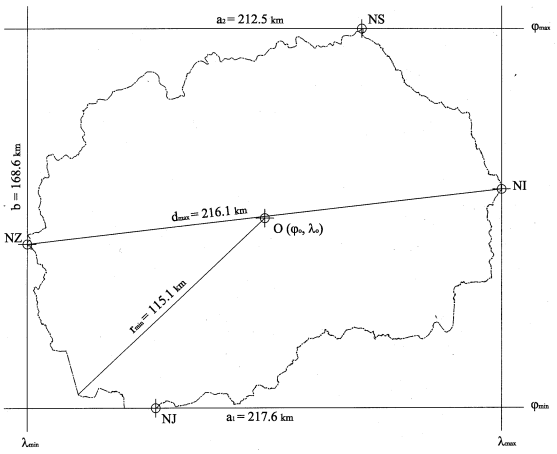

Figure 1. Dimensions and spatial arrangement of the state territory

The territory of the Republic of Macedonia has an ellipsoidal shape, with a gentle elongation in the direction of the parallels.

The spatial arrangement and shape of the national territory indicate suitability for the application of Stereographic and conic projections, while its dimensions allow for the entire territory to be mapped into one coordinate system with satisfactory accuracy.

Research for the selection of the new State cartographic projection begins with analyses of the existing State cartographic projection. The Gauss-Krüger projection was adopted as the State cartographic projection for the Republic of Macedonia in 1924, and its basic properties are well known within the geodetic community [1], [10].

The coordinate system of the projection aligns with the equator, representing the Y-axis, and the meridian with a geographical longitude of $\lambda = 21°$, defining the X-axis of the system. There is constant linear module $m_o = 0.9999$.

Isolines are parallel lines symmetrically arranged concerning the projection of the central meridian.

The results of testing, subject to comparison with the parameters of other projections, point out the shortcomings of the current state cartographic projection. These deficiencies arise from the insistence on mapping the entire national territory into one coordinate system (the seventh), a consequence of the characteristics of the projection and the geographical position of our country. Typically, the part of the territory located east of the meridian 22°30' belongs to the eighth coordinate system.

The insistence on a single coordinate system predicts deformations in the projection ranging from -10 cm/km to 25.5 cm/km, which represents an exceptionally high value.

The second in the series of examined projections is the Tissot projection, serving as the basis for comparing and evaluating the remaining conformal projections in the selection of the new State cartographic projection due to its property of minimizing linear deformations [7].

Although not inherently conformal, the projection is characterized by practical conformality, especially when projecting small territories.

The distribution of linear deformations is regular, and isolines have the shape of concentric ellipses. The maximum accuracy of the projection is achieved by modulating the rectangular coordinates with a linear modulus m = 0.99997, allowing the entire territory of the Republic of Macedonia to be covered with deformations not exceeding ±3 cm/km. This is an absolute minimal value for linear deformations achievable with any of the conformal cartographic projections.

The set of conformal projections, among which the choice for the new State cartographic projection needs to be made, includes:

- Lambert Conformal Conic Projection (Variant V),
- Transverse Mercator Projection,
- Stereographic Projection,
- UTM Projection.

Considering the shape of the national territory, *Lambert's conformal conic projections* stand out as one of the most optimal solutions. This is especially true for Variant V of conformal conic projections, which possesses the property of minimizing linear deformations.

The distribution of linear deformations in this projection is regular, and isolines are represented through projections onto parallels that transform into concentric circles. The coordinate system of the projection is defined by the meridian with a geographical longitude of λo = 21°45', materializing the X-axis, and the tangent to the projection from the parallel with a geographical latitude of φo = 41°36'50", materializing the Y-axis of the coordinate system [5].

The maximum values of linear deformations resulting from the conditions under which the projection is defined are distributed in the range of ±4.4 cm/km.

The *Transverse Mercator projection* shares an identical mathematical foundation and characteristics with the Gauss-Krüger projection.

The central meridian of the projection, materializing the X-axis of the rectangular coordinate system, passes through the center of the national territory, enabling a regular and symmetrical distribution of linear deformations.

Modulating the rectangular coordinates with a constant linear module m=0.99993 allows the entire national territory to be mapped with deformations ranging from -7 cm/km to 7.3 cm/km.

The inclusion of the *Stereographic projection* in the set of examined projections is primarily dictated by the shape of the territory of the Republic of Macedonia. The proper arrangement of linear deformations distributed in the form of concentric circles corresponds entirely to the spatial distribution of the national territory [6].

The center of the Stereographic projection, which simultaneously represents the origin of the rectangular coordinate system, is located at the point with coordinates:

$$\varphi_o = 41^\circ\ 30'\ 30" \quad \lambda_o = 21^\circ\ 45'\ 50"$$

Increased accuracy of the projection is achieved by introducing a secant projection plane, where the rectangular coordinates are modulated with a module m=0.999965. This allows the entire national territory to be covered with deformations not exceeding ±3.8 cm/km.

The last in the series of analyzed projections is the *UTM (Universal Transverse Mercator) projection*. Its significance lies primarily in being an integral part of the World Projection System and a fundamental projection for NATO member countries.

The application of the UTM projection for mapping the territory of the Republic of Macedonia allows adherence to global standards,

particularly in the production of topographic maps [5].

The key characteristics of the UTM projection indicate that it is essentially identical to the Gauss-Krüger projection, differing only in the linear modulus, which here has a value of m=0.9996. This practically means that a negative linear deformation of -40 cm/km is introduced at the central meridian, which is simultaneously the maximum linear deformation for the entire country.

The main characteristics and parameters that appear as criteria for evaluating the projections are presented in Table 1. The analysis of quantitative criteria includes a comparison of characteristics in terms of linear deformations, surface deformations, and meridian convergence:

- The Stereographic projection is characterized by absolute minimal linear deformations. The closest results to it are achieved by the Lambert conformal conic projection, followed by the Transverse Mercator projection, Gauss-Krüger projection, and UTM projection.
- Identical results and order of projections are obtained when analyzing surface deformations.
- The maximum convergence of meridians has the same value for the Transverse Mercator projection and Lambert conformal conic projection. Following them are the Gauss-Krüger projection and UTM projection. The Stereographic projection stands out because it lacks expressions for determining meridian convergence as a function of rectangular and geographical coordinates.

The analysis of qualitative criteria includes other criteria that cannot be mathematically quantified:

- The distribution of linear deformations is regular in all tested projections, except for the Gauss-Krüger projection and the UTM projection, where asymmetry occurs due to the mismatch of the central meridian with the mathematical-geographical positi-on of the Republic of Macedonia.
- The analysis of the mathematical models of the test projections is of interest. Lambert's Conformal Conic projection has the simplest expressions, followed by the Gauss-Krüger projection and the Transverse Mercator projection. The UTM projection, due to its complex surface marking system, lags in this criterion, while the Stereographic projection has the most complex mathematical apparatus.
- The cylindrical conformal cartographic projections, followed by Lambert's conformal conic projection, have the most comprehensive mathematical models. In the Stereographic projection, some expressions for basic calculations are missing.
- The tradition of use in the Republic of Macedonia is on the side of the Gauss-Krüger projection, which has been our national cartographic projection for over 100 years. Due to the identical mathematical models, the Transverse Mercator projection and the UTM projection will follow the Gauss-Krüger projection. The application of Lambert's conformal conic projection in the Republic of Macedonia is

Table 1. Basic characteristics of the test projections [8].

Criteria \ Projection			Gauss-Krüger		Tissot		Lambert conical	Transverse Mercator		Stereographic		UTM
			tangent	secant	tangent	secant		tangent	secant	tangent	secant	
Quantitative	Linear deformations	Max. (cm/km)	+35.4	+25.4	+6.0	±3.0	±4.4	+14.3	+7.3	+7.3	+3.8	-40.0
		Θ_l (test-model) (cm/km)	8.0	8.0	2.3	1.3	2.9	3.7	4.3	2.8	1.7	32.0
		Θ_l (cities) (cm/km)	10.4	8.5	2.4	1.2	2.8	4.4	3.8	3.1	1.5	29.5
	Area deformations	Max. (m^2/ha)	7.1	5.1	1.2	0.6	0.9	2.9	1.5	1.5	0.8	-8.0
		Θ_p (test-model) (m^2/ha)	1.6	1.6	0.5	0.3	0.6	0.7	0.9	0.6	0.3	6.4
		Θ_p (cities) (m^2/ha)	2.1	1.7	0.5	0.2	0.5	0.9	0.8	0.6	0.3	5.9
	Max. convergence		+1° 21' 26.73"		+0° 51' 40"		-0° 51' 26.54"	+0° 51' 29.43"		-0° 51' 54"		+1° 21' 26.7"
Qualitative	Distribution of linear deformations		irregular - asymmetric		regular - ellipses		regular - arcs	regular - lines		regular - circles		irregular - asymmetric
	Mathematical model		relative complex		complex		simple	relative complex		complex		complex - labelling
	Model completeness		complete		incomplete		complete	complete		incomplete		complete
	Tradition in RM		maximum		none		none	maximum		none		moderate
	Economical aspects		none		-		maximum	basic		maximum		increased
	European standards		8% from European countries use as SCP		0% from European countries use as SCP		14% from EU countries use as SCP	61% from European countries use as SCP		8% from European countries use as SCP		8% from EU countries use as SCP

limited to the Civil Aviation Sector. The Stereographic projection does not have a tradition of use in our country.

- According to economic aspects, it is considered that the use of the existing national cartographic projection will not incur additional costs. Considering that it is a projection with a well-known mathematical apparatus, the choice of the Transverse Mercator projection should only incur basic costs necessary for transfor-ming the entire set of spatial data. In contrast, the introduction of the UTM projection, in addition to basic costs, would incur additional (not significant) costs for the education of the professional staff regarding the surface marking system. The most significant additional education costs would be realized if Lambert's conformal conic projection or the Stereographic projection were chosen as the new national cartographic projection.
- Regarding European standards in the field of national cartographic projections, the situation is quite clear. The Transverse Mercator projection has by far the greatest application, followed by Lambert's conformal conic projection, UTM projection, Gauss-Krüger projection, and the Stereographic projection.

Taking into account the analysis conducted, a table can be compiled in which the assessments for the test projections will be systematized in terms of the established criteria. For this purpose, the standard methodology for evaluating the projections was used, in which the weighting of the each criteria was applied for each of the projections (5 points - the best projection, 1 point - the worst projection).

From the results in Table 1, the Transverse Mercator projection clearly stands out as the best choice for a new state cartographic projection for the needs of the national survey and official cartography. While it may have weaker results in some mathematical criteria compared to the Stereographic projection and Lambert Conformal Conic projection, this projection demonstrates excellent performance in qualitative criteria due to its close resemblance to the Gauss-Krüger projection. The widespread use of this projection in most European countries further confirms its favorable characteristics.

The Lambert Conformal Conic projection exhibits excellent properties in terms of mathematical criteria and solid properties in qualitative criteria. However, further investigation is needed to assess its potential use as the official cartographic projection for aerial navigation.

The inadequacy of the Gauss-Krüger projection concerning the mathematical-geographical position of the Republic of Macedonia excludes this projection from the competition for retaining the status of the state cartographic projection. Its primary advantage lies in its extensive tradition of use in our country.

Regarding the UTM projection, it occupies the second-to-last place in our analysis. Its only advantage lies in the alignment of the state cartographic projection with the official cartographic projection for the production of topographic maps according to NATO standards.

Table 2. Evaluation of test projections [8].

Projection / Criteria	Gauss-Krüger	Lambert conical	Transverse Mercator	Stereographic	UTM
Linear deformations	2	4	3	5	1
Surface deformations	2	4	3	5	1
Meridian convergence	3	5	5	1	3
Linear deform. distribution	1	5	5	5	1
Mathematical model	4	5	4	1	2
Completeness of the model	5	2	5	1	5
Tradition in RM	5	2	4	1	3
Economic aspect	5	2	4	1	3
European standards	2	4	5	1	3
Overall	29	33	38	21	22

However, this is not sufficient (considering the series of drawbacks) for the UTM projection to take the place of the new State Cartographic Projection.

In conclusion, despite being characterized by minimal linear and surface deformations, the Stereographic projection, due to the remaining criteria, especially qualitative ones, lags behind the other projections in the set of tested projections for the needs of establishing a new State Cartographic Projection.

3. CONCLUSIONS

Based on all the information presented so far, the conclusion is evident that the **Transverse Mercator projection** represents the best choice for a new State cartographic projection in the Republic of North Macedonia, catering to the needs of national mapping and official cartography.

Of course, it should be noted that the introduction of the new State cartographic projection must be considered in inseparable unity with the introduction of **the new geodetic datum** for the territory of the Republic of Macedonia.

4. REFERENCES

[1] Borčić B. (1955): "Mathematical Cartography (cartographic projections)", Technical book, Zagreb.

[2] Jovanovic V. (1983): "Mathematical Cartography", VGI, Belgrade.

[3] Srbinoski Z. (2001): "Enclosure to research on defining a new state cartographic projection", Doctoral dissertation, University "St. Cyril and Methodius ", Skopje.

[4] Srbinoski Z., Bogdanovski Z. (2017): "Lambert normal conic projection with two standard parallels for territory of Republic of Macedonia", Scientific Journal of Civil Engineering, Vol. 6, Iss. 1, pp. 19-23.

[5] Srbinoski Z., Bogdanovski Z. (2017): "World projecting system - standards and usage", Scientific Journal of Civil Engineering, Vol. 6, Iss. 2, pp. 135-141.

[6] Srbinoski Z., Bogdanovski Z., Kasapovski F., Gegovski T. (2018): "Stereographic projection for territoriy of the Repubilc of Macedonia", Scientific Journal of Civil Engineering, Vol. 7, Iss. 2, pp. 35-42.

[7] Srbinoski Z., Bogdanovski Z., Kasapovski F., Gegovski T. (2018): "Tissot compensation projection for the Repubilc of Macedonia", Scientific Journal of Civil Engineering, Vol. 8, Iss. 1, pp. 27-34.

[8] Srbinoski Z. (2019): "Study on the selection of a new state cartographic projection", Agency for Real Estate Cadastre, Skopje.

[9] Srbinoski Z., Bogdanovski Z., Kasapovski F., Gegovski T., Petrovski F. (2022): "Transverse Mercator projection for the territory of Macedonia", Scientific Journal of Civil Engineering, Vol. 11, Iss. 2.

[10] Srbinoski Z. (2023): "Mathematical Cartography", Faculty of Civil Engineering - Skopje.

Goce Taseski
PhD, Associate Professor
Ss. Cyril and Methodius University in Skopje
Faculty of Civil Engineering
N. Macedonia
taseski@gf.ukim.edu.mk

Nikola Krstovski
MSc, Associate
Ss. Cyril and Methodius University in Skopje
Faculty of Civil Engineering
N. Macedonia

APPLICATION OF SWMM FOR CAPACITY ANALYSIS OF COMBINED SEWER SYSTEM

A sewer system is an underground infrastructural facility that is designed to receive storm and sanitary water and safely distribute it within urban areas. The distribution of this water can be accomplished through separate and combined sewer systems. In separate sewer systems, sanitary and stormwater flow through different pipes, while in combined sewer systems, they flow through the same pipe.

In the past, designing a sewer system was a tough and complex task due to all calculations being done by hand. However, with the advancement of technology and computers, numerous software programs have been developed for flow simulation in sewer systems. These software applications can now be utilized to create hydraulic models for planned sewer networks, enabling calculations of pipe dimensions, as well as to assess the flow capacity of existing sewer networks.

The objective of this topic is to assess the flow capacity of the existing sewer network in the city of Bitola using EPASWMM (Storm Water Management Model).

Keywords: combined sewer system, hydraulic model, rational method, SWMM

1. INTRODUCTION

The flow rate in a combined sewer system can vary significantly throughout the year. During dry periods, the flow rate is zero, whereas during heavy rainfall events, it can reach very high values. It is crucial to accurately determine the volume of water that the sewer system can accommodate, considering both functional and economic factors. If the network is undersized, it won't be able to handle the surface water, resulting in water overflow on the streets and the formation of watercourses, which could potentially lead to loss of life. On the other hand, if the sewer network is oversized, it would mean unnecessary expenditure on construction. Hence, accurately determining the water volume is of utmost importance for sizing the sewer system.

2. RATIONAL METHOD

The Rational method was developed approximately 130 years ago by Kuichling (1889). The rational method is based on a simple formula that relates runoff- producing potential of the catchment area, the average intensity of rainfall for particular length of time (time of concentration) and the catchment area. This method is applied when the size of the catchment area is less than 15 km2. The equation is:

$$Q = F \cdot C \cdot i \qquad (1)$$

- F – catchment area [ha]
- i – rainfall intensity [l/s/ha]
- C – runoff coeficient

The runoff coefficient C, is a dimensionless ratio intended to indicate the amount of runoff generated by the catchment area, given an average intensity of precipitation for a storm. The value of this coefficient varies between 0.05-0.95, depending on the type of the catchment area.

Storm intensity i is a function of geographic location and design exceedence frequency (or return interval). The relation between the three components - storm duration, storm intensity, and storm return interval, is presented by a family of curves called the intensity-duration-frequency curves, or IDF curves. They can be determined by analysis of storms for a particular site (Figure 1)

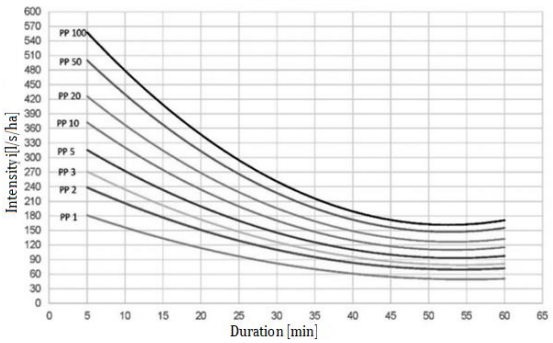

Figure 1. IDF curve

Two key parameters on which peak flow depends are the time of concentration (tc) and the duration of rain (td).

The runoff hydrograph obtained by the rational formula has a triangular shape (Figure 2).

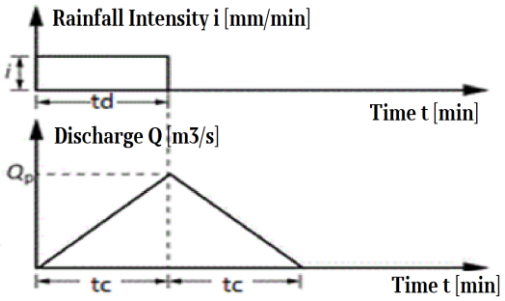

Figure 2. Hydrogram obtained using the Rational Method

The time of concentration (tc) is defined as the time it takes for water drops from the furthest point in the catchment to reach the specified profile. When the duration of rainfall (td) is less than tc (td < tc), the maximum flow will be lower because the entire catchment area does not contribute to flow formation (Figure 3a). On the other hand, when td > tc, the flow will increase up to a maximum value and then gradually decrease (Figure 3b). The maximum flow occurs when td = tc because the entire catchment area actively participates in flow formation, and the rainfall duration is shorter compared to previous cases. Shorter-duration rains have higher intensities, resulting in higher maximum runoff.

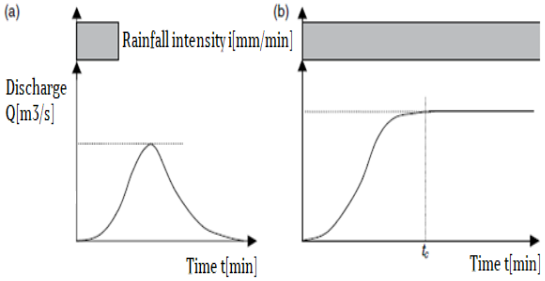

Figure 3. Runoff hydrograph (a - td<tc; b – td>tc)

The time required for water to reach the analyzed profile (tc) can be divided into two components:

$$t_c = t_1 + t_2 \qquad (2)$$

- t_1 – time required for water to reach the channel
- t_2 - time of water flow through the channel itself

The time of water entering the sewer network depends on various factors such as the slope of the terrain, the type of surface, the distance to the drain, the infiltration characteristics of the soil, and more. A common approach to estimating this time is as follows:

- t_1=5 [min] - for impervious surfaces, particularly in densely populated cities with closely spaced catchments
- t_2=10-15 [min] - for densely populated urban cities with low terrain slope
- t_3=20-30 [min] - for residential zones with widely spaced sinks

3. EPA SWMM

EPA SWMM is a dynamic, physically based model that simulates the process of transformation of precipitation into runoff. It can be used for a single event or a longer-term simulation of the quantity and quality of runoff water, most often from urban areas.

This software was developed by the US EPA (Environmental Protection Agency) in 1971. It is very often used in the stages of planning, analysis and design of sewage systems for the acceptance of atmospheric and waste waters, culverts under the road, open channels, etc. SWMM allows data input in a virtual environment and then based on that data input makes hydrological, hydraulic and water quality simulations, as well as reviews the obtained results in different formats.

The SWMM takes into account the various hydrological processes that affect runoff, such as:

- irregularity of rainfall
- snow melting
- water retention in surface depressions
- evaporation
- infiltration of the rain in the unsaturated layers of the soil
- interaction between collectors and groundwater

The capabilities of SWMM for hydraulic modeling of flow through pipes, channels, reservoirs or through flow distribution facilities are as follows:

- Collector network of unlimited size
- Possibility of using various forms of open and closed channels
- Modeling of special facilities such as reservoirs, water treatment facilities, flow distribution facilities, pumps, overflows, etc.
- Application of kinematic and dynamic wave methods for calculation of flow in pipes
- Modeling of different flow regimes, such as free water mirror flow, pressurized flow, reverse flow, surface water retention, etc.
- Modeling the operation of the pump, the openings and the crown level of the spillway

The working concept of SWMM is based on the interaction of several main components of the environment, which are modeled as objects. Those components and objects are:

- Atmosphere, from which rain or snow falls and pollutants that settle on the surface of the land. SWMM uses the Rain Gage tool to represent precipitation as an input to the system.
- Land surface, which is represented through one or more Sub-Catchment objects. It receives precipitation from the atmosphere, which can be in the form of rain or snow. From the land surface, a part of the runoff goes into the groundwater through infiltration, and the rest into the transport system as surface runoff and pollution
- Groundwater receives infiltration from the Land Surface and transfers a part of this inflow to the Transport systems. This is modeled using Aquifer objects
- The transport system contains a network of transport elements (channels, pipes, pumps and stoppers), collection elements and treatment elements that transport the water to an outlet in a recipient or a treatment facility. Inflows to this component can come from surface runoff, groundwater interflow, sanitary dry weather flow, or from user-defined hydrographs. The components of the Transport system are modeled with Node and Link objects.

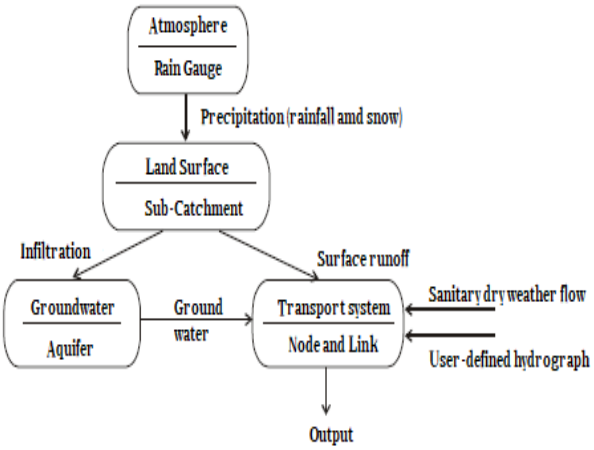

Figure 4. SWMM conversion of precipitatiton to flow

4. HYDRAULIC MODEL

The case study being analyzed involves the existing combined sewer network in the city of Bitola.

The hydraulic model of the existing sewerage network in the city of Bitola was created using the software package called "Storm Water Management Model" (SWMM).

The data for the manholes and pipes used in the hydraulic model were obtained from the public utility company 'Niskogradba'. A total of 4215 manholes were imported into the model. The pipes in the secondary network have diameters ranging from 200 mm to 500 mm, while the collectors have diameters varying from 500 mm to 2200 mm. The sewerage network is composed of 7 main collectors with a total length of approximately 21 km.

The total catchment area for the sewerage network in Bitola is 1025 hectares, which is distributed across 32 separate catchment areas (Figure 5). These catchment areas are relatively large in size. Using the Thiessen method, each catchment area is further divided into sub-catchment areas assigned to individual manholes. This means that each manhole has its own designated catchment area, where atmospheric water flows and contributes to the overall drainage system flow rate.

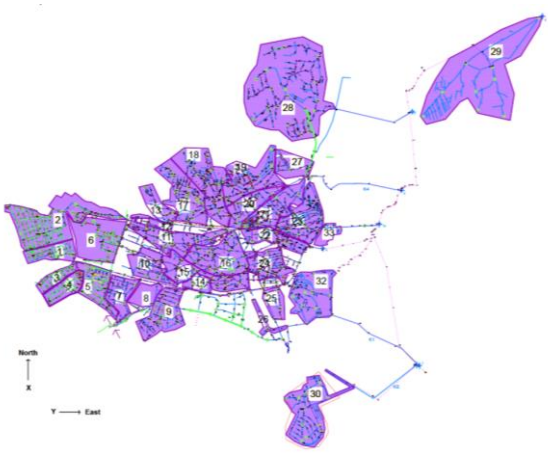

Figure 5 Hydraulic model of the sewerage network in the city of Bitola

The runoff coefficient for each catchment area is determined separately, depending on the percentage of greenery, roof, asphalt and concrete. The following runoff coefficients are adopted depending on the type of surface:

- 0.90 - runoff coefficients for roofs
- 0.80 - runoff coefficients for asphalt surface
- 0.70 - runoff coefficients for concrete surface
- 0.25 - runoff coefficients for parks

Based on the information provided by the public utility company, three overflow points were incorporated into the hydraulic model. Specifically, two overflow points were placed along collector 4, and one overflow point was placed along collector 3. These overflow points serve as outlets for excess water in the event of high flow conditions in the sewer network.

The maximum amount of sanitary wastewater for each catchment area is obtained from the public utility company and it ranges from 0.2 (l/s/ha) to 2 l/s/ha.

During the hydraulic analysis, rain with a return period of 2 years, intensity of 93.02 l /s/ ha and duration of 20 minutes was used.

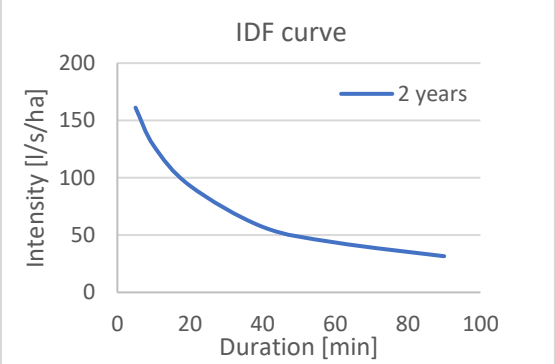

Figure 6. IDF curve used in SWMM

5. ANALYSIS OF THE RESULTS FROM THE HYDRAULIC MODEL

The results obtaioned from the hydraulic model are shown in the Figures 7-9. The hydraulic analysis of the sewage network in Bitola reveals the presence of bottlenecks in a specific section of the network, resulting in water spills during rain events with an intensity of 93.02 (l/s/ha). Additionally, a significant portion of the sewerage network exhibits underutilization of pipe cross-sections, indicating the presence of oversized pipes.

Table 1 shows the length of the pipes and utilization of the capacity of the pipes expressed in %.

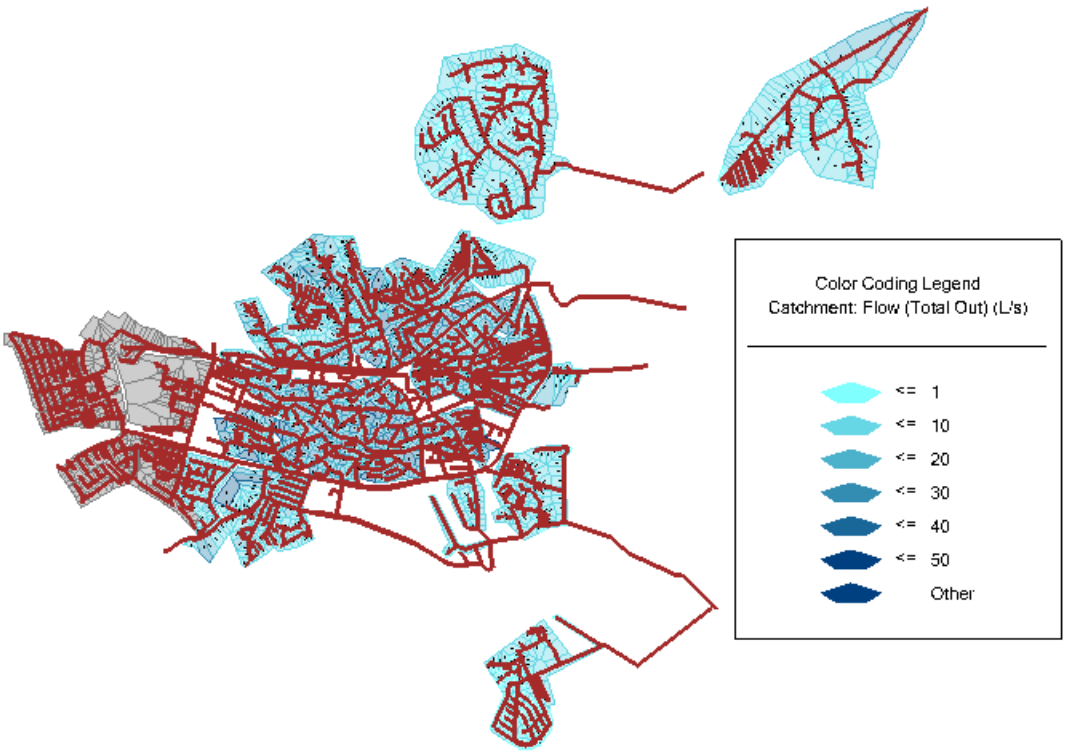

Figure 7. Catchment flow (Total out)

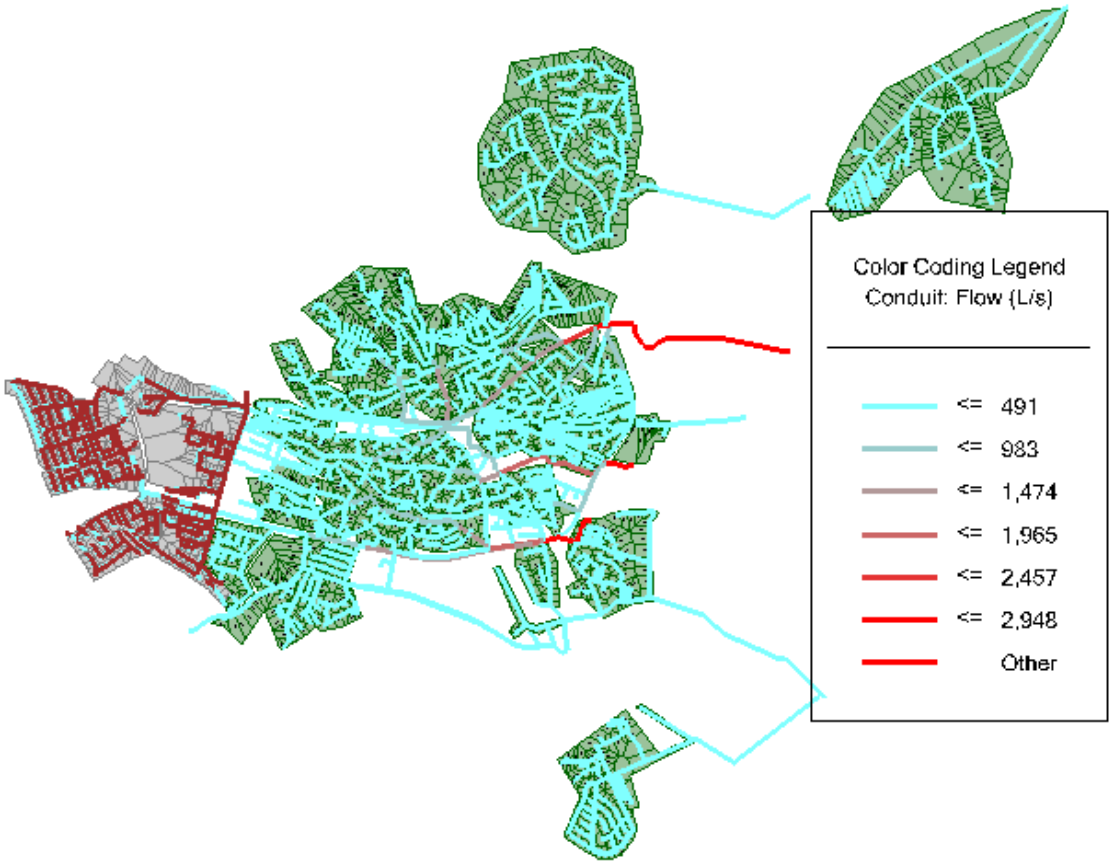

Figure 8. Conduit flow

.

Figure 9. Flow/Capacity of the sewer system

Table 1. Utilization of the capacity and pipe length

Flow/Capacity [%]	Pipe length [km]
<50	141.4
50-80	11.1
80-100	4.3
>100	7.6

6. CONCLUSION

SWMM is a modern method of designing sewer network, which with the help of the power of computers can very quickly simulate stormwater, turning it from rain into canal water, taking into account the topography of the terrain, the slope of the conduits, the type of surface, etc. The advantage of this method is that can solve very complex sewer networks and in a very easy way make changes in them. The great advantage of this method is that the model can be calibrated, i.e. the input parameters can be changed and thus we can get a model that works approximately the same as the real sewer network.

With the application of such software, sewerage networks can be designed in which the utilization of the cross-section of the pipe will be within the allowed limits, that is, we will not even have an oversizing of the sewerage network, which would mean unreasonably spent finances for the construction of that network or undersizing on the pipes, which would lead to spillage of water from the sewers even during minor rains.

REFERENCES

[1] Nikola Krstovski, “DIFFERENT ANALYSIS METHODS FOR STORMWATER SYSTEM MODELING” Master thesis, Skopje, Macedonia, 2022.

[2] Rossman LA. Storm water management model user’s manual, version 5.0, EPA. United States. 2009; p. 233.

[3] Junaidi, A.; Ermalizar, L.M. (2018): “Flood simulation using EPA SWMM 5.1 on small catchment urban drainage system”.

[4] Waikar, M.L.; Undegaonkar Namita, U. (2015): “Urban Flood Modeling by using EPA SWMM 5”.

[5] David B. Thompson “The Rational Method”, September, 2006, Civil Engineering Department, Texas Tech University.

Marija Vitanova
PhD, Associate Professor
Ss. Cyril and Methodius University in Skopje
Institute of Earthquake Engineering and Engineering Seismology
N. Macedonia
marijaj@iziis.ukim.edu.mk

Igor Gjorgjiev
PhD, Full Professor
Ss. Cyril and Methodius University in Skopje
Institute of Earthquake Engineering and Engineering Seismology
N. Macedonia

Nikola Naumovski
PhD, Assistant
Ss. Cyril and Methodius University in Skopje
Institute of Earthquake Engineering and Engineering Seismology
N. Macedonia

Viktor Hristovski
PhD, Full Professor
Ss. Cyril and Methodius University in Skopje
Institute of Earthquake Engineering and Engineering Seismology
N. Macedonia

ENVIRONMENTAL INFLUENCES ON BRIDGES: AN ASSESSMENT STUDY

Environmental conditions resulting from climate change may have diverse impacts on the safety and performance of infrastructure. Bridges, as pivotal structural components of transportation systems, are subject to various natural and environmental factors. Therefore, periodic definition of their dynamic characteristics, such as natural frequencies through experimental measurements, is crucial for promptly and accurately assessing their current state. In this study, experimental analysis is employed for this purpose, involving the measurement of structural responses under ambient conditions. This paper presents an investigation into the environmental effects on the dynamic characteristics of reinforced concrete (RC) frame bridges. The study focuses on two overpasses with similar geometries. Three sets of measurements were conducted for each overpass: in October 2017, March 2020, and May 2022. The identified dynamic characteristics were compared across different time points and correlated with environmental effects. The analysis results indicate that the identified natural frequencies effectively reflect changes in the dynamic characteristics of the overpasses due to environmental effects. A significant difference in identified natural frequencies is observed in the longitudinal direction, while minimal variation occurs in the vertical direction.

Keywords: ambient vibration measurements, dynamic characteristics, reinforced concrete bridges, condition assessment

1. INTRODUCTION

Bridges are inevitably exposed on the daily, seasonal, and annual air temperature variations which affects the characteristics of the structures. During their service life, local damage can be reflected by the changes in dynamic properties. Therefore, a successful damage assessment relies heavily on the prediction accuracy of the dynamic properties. The variations of modal parameters caused by environmental factors are very significant and often greater than those caused by structural damage [1] or normal loads [2]. The periodic (diurnal, seasonal, and yearly) and transient temperature variations always mask changes in

dynamic properties due to actual damage. Recently, more research has focused on the effect of temperature on the dynamic properties of bridges [3].

In practice, the effect of temperature variations on structural dynamic properties have been attributed to the reasons outlined below. First, structural deformations occurred with variations in temperature-varying environments and were called large deformation effects [4]. Second, structural stiffness changed because of thermal stress in the well-known stress stiffening effect [5]. In addition, material properties were temperature dependent; for example, the decrease in the elastic modulus of concrete and of steel led to a reduction in modal frequencies. Furthermore, and equally important, the elastic properties of support (especially for bridge structures) were more easily affected by thermal variations, and at low temperature, the boundary conditions also changed suddenly [6]. Accordingly, the factors that affected the dynamic properties of bridge structures were complex and led to some specific damage detection methods, such as technology that does not need estimations of the modal parameters [7]. In addition, a thermal performance study of bridges based on long-term monitoring data still piqued researcher interest [8]; however, the cost of the health monitoring system was high, despite increasingly more advanced structural health monitoring (SHM) technologies [9]. To remove the environmental impacts, regression-based analysis [10] and principal component analysis [11] were adopted, but these analyses were data-driven black box modeling techniques. Although Zhou and Song [12] proposed a physics-based environmental-effects-embedded model updating method to overcome these shortcomings, the selection of the updating parameters was also critical, and a large deflection effect was not taken in account.

In the present study, time-varying thermodynamic properties of 2 span girder bridges were analyzed and compared.

2. RESEARCH METHOD

2.1 MEASURING EQUIMPMENT

The dynamic characteristics have been determined by measurements of ambient vibrations. The equipment with an acquisition system that was used to take the measurements, is sensitive accelerometers that have recorded the records. In this case PCB Piezotronics devices, model 393B12, manufactured by National Instruments with a sensitivity of 10,000 mV and a range of up to 4.9 m/sec^2, with a size of 0.5g were used. Data acquisition was performed with the acquisition system - module NI cDAQ-9178 and 4 NI 9234 boards (Fig. 1). The recorded acceleration measurements are expressed in "Earth acceleration - g" (9.81 m/sec^2).

Figure 1. Field monitoring equipment (left), three-way accelerometer (right)

The measurements were carried out using a sampling rate of 2.048 Hz. In total, 15 accelerometers were used with various measurement locations and directions. During the measurements, the sensors were placed in the different points of the bridge: in the middle of the bays and above the piers. During all measurements, one accelerometer was located in a reference point in order to enable the comparison of the amplitudes of the other sensors with the reference points for defining the tonal forms of vibration. These measurements cover a frequency range from 0 to 40 Hz, where the first resonant frequencies are found. The processing of the record was carried out by applying a fast Fourier transformation so that it was possible to define the frequency composition of the registered vibration from which the natural frequencies of the objects could be identified.

2.2 MEASURING PROCEDURE

Withing the framework of this research, field measurements of two overpasses (OP2 and OP3, Fig. 2) were carried out. The selected bridges are located over the "Friendship" highway, Demir Kapija - Gevgelija section, designed according to modern regulations that consider the seismic action. Both overpasses are with 2 spans each of which 23 m. The selected bridges are designed according to modern regulations that consider the seismic action. The initial measurements of the structures were carried out in October 2017,

during which the trial loading of the bridges with static and dynamic loads was performed.

Figure 2. Measured structures OP2 and OP3

The load capacity and deformability of the built construction is compared with the results of the design project. The precision of the performance and the geometry of the elements were checked, and the quality of the incorporated materials and thus the usability of the construction was checked. At the beginning of March 2020, additional measurements were performed on the bridges with a duration of 10 min. The same measurements were repeated in May 2022. The two bridges were still not into use. Therefore, only the environmental conditions are the external factors that may effect the dynamic properties of the bridges. For performing the measurements, 15 accelerometers were used, in 5 places, 3 each in the longitudinal x direction, the transverse y direction and the vertical z direction, and they were placed on the edge of the upper structure, in the field and above the middle support (Fig. 3). During the first measurement, the accelerometers were placed on the part of the upper construction, in the direction of Skopje, while during the second measurement, they were placed in the direction of Gevgelija, with the first accelerometer as a benchmark during both measurements being placed in the same place.

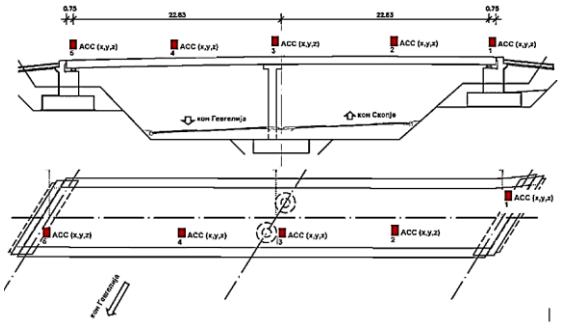

Figure 3. Position of accelerometers on the measured bridge at base and cross-section

2.2.1 Modal damping estimation methods

The methods available to perform identification of modal parameters (in this case modal damping, but it is the same for all modal parameters) of dynamic systems based on their response to ambient excitation are classified as frequency domain or time domain methods. The frequency domain methods start from the output spectrum of half- spectrum matrices estimated from the measured outputs. After obtaining the frequency response curves of the analysed system, modal damping can be measured using half-power bandwidth method and Enhanced Frequency Domain Decompositon (EFDD) method. The half-power bandwidth method consists of locating the resonant frequency and two nearby frequencies f1 and f2 located in the frequency spectrum by application of equation 1:

$$\xi = \frac{f_2 - f_1}{2f_r} \times 100\% \qquad (1)$$

Enhanced Frequency Domain Decompositon was performed in order to calculate the damping (IRF) by using the impulse response of a single degree of freedom. Once a set of points with similar singular vectors is selected for a particular mode (Fig. 4a), this segment of an auto-spectrum may be converted to a time domain (Fig. 4b).

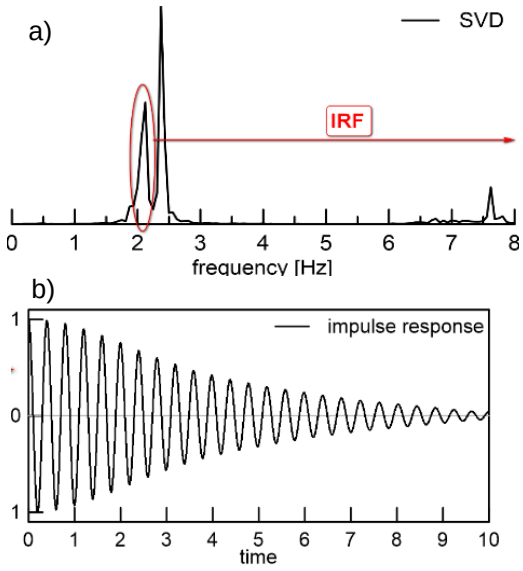

Figure 4. FDD method, estimation of the modal damping ratio

An auto-correlation function with the contribution of a single mode is obtained. As the output correlation of a dynamic system excited by white noise is proportional to its impulse response, it is possible to estimate the modal damping coefficient. This can simply be performed by fitting an exponential function to the relative maxima of the correlation function and extracting the modal damping ratios from the parameters of the fitted expression taking into account the classical expression for the

impulse response of a single degree of freedom.

2.2.2 OP2 Results

Using the previously described procedure, most of the records were obtained at individual points of the investigated bridge. Based on these registrations and their singular value of spectral densities, a certain amount of data on the dynamic characteristics of the investigated structures were obtained. Below, on Fig.5 the curves of singular value of spectral densities for OP2 are presented.

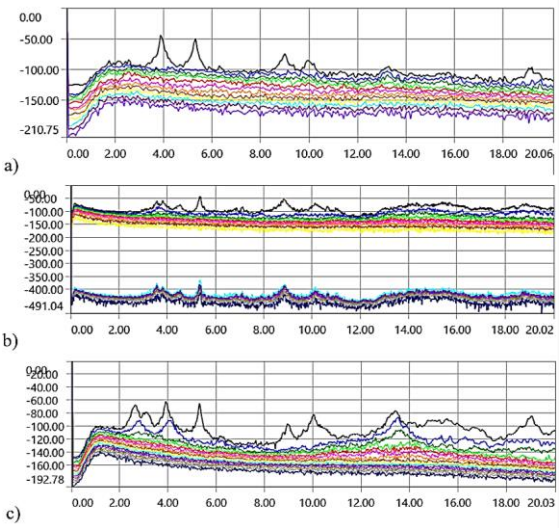

Figure 5. Singular value of spectral densities for OP2 a) 2017, b) 2020, c) 2022

Table 1 shows the frequencies obtained from all measurements, when the accelerometers were placed on the part of the upper construction in the direction of Skopje (measurement 1). From the obtained results, it can be concluded that almost all accelerometers that measured the acceleration in a certain direction show similar results, that is, for longitudinal direction, the frequency is 2.58Hz for 2017year, 3.58 for 2020year and 2.65Hz for 2022.

Table 1 Natural frequencies of the structure for OP2

Mode	Direction	Frequency [Hz]		
		2017	2020	2022
1	Longitudinal	2.58	3.58	2.65
2	Transversal	2.97	3.80	3.12
3	Vertical	3.88	3.81	3.91

It can be seen that the frequency has increased in 2020 and in 2022 came back. In the Transversal direction, the frequency of the structure is 2.97Hz for 2017year, 3.80 for 2020 and 3.12Hz for 2022. In the vertical direction, the frequency of the structure is 3.88Hz for 2017, 3.81 for 2020 and 3.91Hz for 2022. In this direction, the frequency decreased in 2020 and then in 2022 increased to 3.91Hz.

Table 2 shows the damping for each frequency by two methods: half power and IRF. In general, the damping calculated by the two methods corelates with each other. For the first frequency in the vertical direction, the damping is within the range of 0.88% for 2017, 0.73% for 2020 and 1.25% for 2022. For the first frequency in the longitudinal direction, the damping is within the range of 0.71% for 2020 and 3.3% for 2022.

Table 2. Modal damping [%] for OP2

No.	2017			2020			2022		
	Freq.	Half Power	IRF	Freq.	Half Power	IRF	Freq.	Half Power	IRF
1 (V)	3.88	0.80	0.88	3.81	0.37	0.73	3.91	0.73	1.25
2 (V)	5.31	0.58	0.64	5.40	0.39	0.46	5.32	0.40	0.45
3 (L)	2.58	n/a	n/a	3.58	0.54	0.71	2.65	2.43	3.3

V (vertical)
L (Longitudinal)

Fig. 6 presents in more clear way, the difference between the modal damping for OP2 calculated in 2017, 2020 and 2022 according to half power and IRF methods.

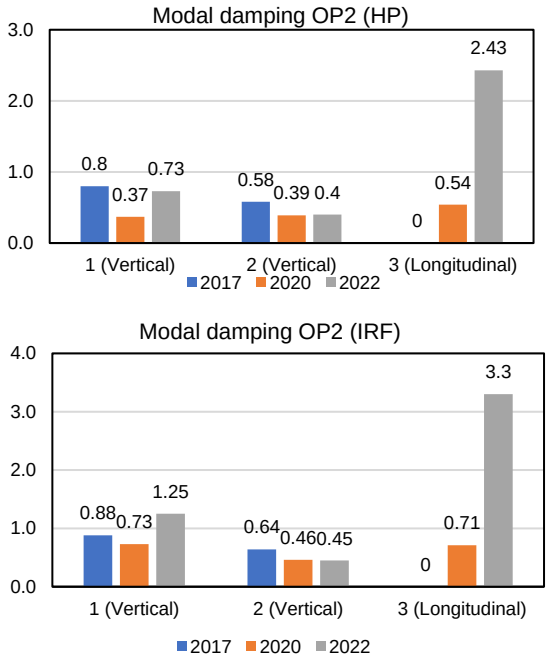

Figure 6 Modal damping [%] for OP2

2.2.3 OP3 Results

Using the same procedure za OP2, all records were obtained at individual points of the investigated bridge. Based on these

registrations and their singular value of spectral densities, a certain amount of data on the dynamic characteristics of the investigated structures were obtained. Below, on Fig. 7 the curves of singular value of spectral densities for OP3 are presented.

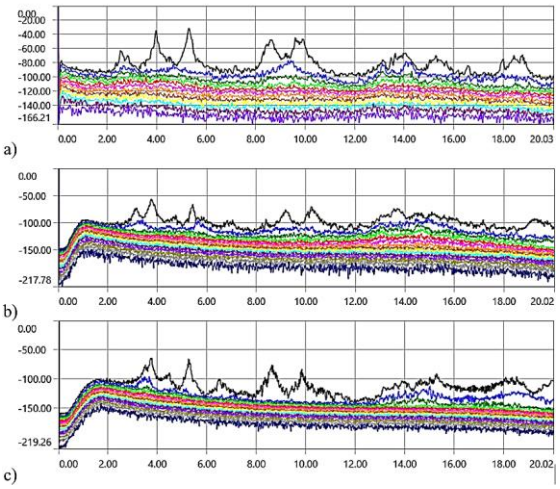

Figure 7. Singular value of spectral densities for OP3 a) 2017, b) 2020, c) 2022

Table 3 shows the frequencies obtained from all measurements, when the accelerometers were placed on the part of the upper construction in the direction of Skopje (measurement 1) for bridge OP3. From the obtained results, it can be concluded that almost all accelerometers that measured the acceleration in a certain direction show small differences in natural frequencies. For longitudinal direction, the frequency is 2.53Hz for 2017 year, 3.14 for 2020 year and 3.50Hz for 2022. It can be seen that the frequency has continuously increased in 2020 and in 2022. In the Transversal direction, the frequency of the structure is 2.84Hz for 2017 year, 3.49 for 2020 year and 3.77Hz for 2022. In the vertical direction, the frequency of the structure is 3.98Hz for 2017 year, 3.78 for 2020 year and 3.78Hz for 2022. In this direction, the frequency decreased in 2020 and continued with same value till 2022.

Table 3. Natural frequencies of the structure for OP3

Mode	Direction	Frequency [Hz]		
		2017	2020	2022
1	Longitudinal	2.53	3.14	3.50
2	Transversal	2.84	3.49	3.77
3	Vertical	3.98	3.78	3.78

Table 4 shows the damping for each frequency by two methods: half power and IRF. In general, the damping calculated by the two methods corelates with each other. For the first frequency in the vertical direction, the damping is within the range of 0.78% for 2017, 1.44% for 2020 and 1.06% for 2022. For the first frequency in the longitudinal direction, the damping is within the range of 0.82% for 2017 and 2.18% for 2020.

Table 4. Modal damping [%] for OP3

No.	2017			2020			2022		
	Freq.	Half Power	IRF	Freq.	Half Power	IRF	Freq.	Half Power	IRF
1 (V)	3.98	0.59	0.78	3.78	1.15	1.44	3.78	1.06	1.06
2 (V)	5.28	0.61	0.84	5.35	0.49	0.65	5.27	0.25	0.62
3 (L)	2.58	0.69	0.82	3.14	2.02	2.18	3.50	n/a	n/a

V (vertical)
L (Longitudinal)

In more clear way, Fig. 8 presents the difference between the modal damping for OP3 calculated in 2017, 2020 and 2022 according half power and IRF methods.

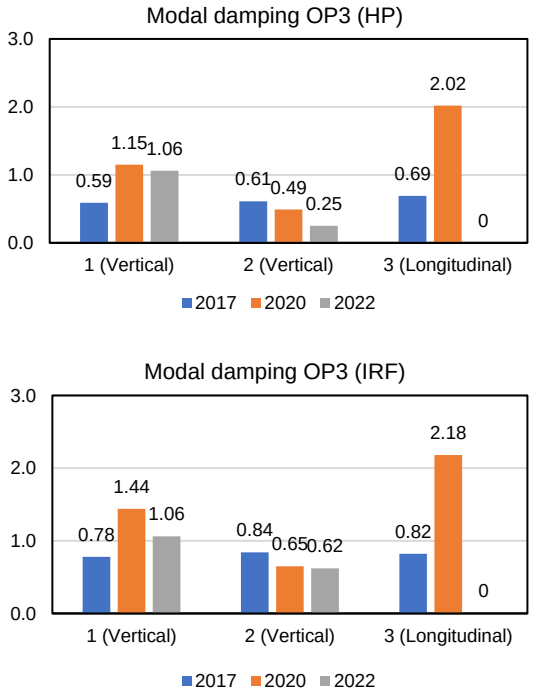

Figure 8 Modal damping [%] for OP3

3. WEATHER CONDITIONS

Engineering materials change their properties and are vulnerable to damage from the surrounding environment, whether they are concrete, steel, or wood. Some environmental factors are considered during structural design, primarily in terms of stress conditions. However, the changes in fundamental environmental conditions such as temperature and humidity can be challenging because they may influence structural dynamic properties. Environmental monitoring is therefore an

essential component of this bridge measurement program. The monitoring program involves gathering information on temperature, humidity, and environmental data analysis. Because the object region has a limited number of monitoring sensors, a relatively good profile of the environmental conditions was constructed by collecting monitored data for at least 6 months before the bridge measurements. The weather monitoring was conducted for the years 2017, 2020 and 2022. The most essential information to consider in these records will be the extremes in averages of temperature and humidity.

3.1 TEMPERATURE

According to the monitored program, the regularly collected set of data was grouped into three monitoring periods. The first monitoring period was a period of one month before the bridge measurements, while the second monitoring period was a period of three months prior to the measurements. The last analyzed period was a period of six months before the structure's measurements. The determination of real temperature inside each structural part was not conducted because the measurements were only for ambient temperature. As a result, it was decided to evaluate how these conditions might affect the structural dynamic characteristics.

Table 5 Temperature observation for period of 1 month before bridge measurements

Year	Avg Max [O]	Avg Mean [O]	Avg Min [O]	Max [O]	Min [O]
2017	23.7	15.7	8.3	37	-3
2020	13.3	6.5	0.3	25	-6
2022	23.1	15.2	7.5	34	-2

Table 6 Temperature observation for period of 3 months before bridge measurements

Year	Avg Max [O]	Avg Mean [O]	Avg Min [O]	Max [O]	Min [O]
2017	28.6	20.5	12.3	40	-3
2020	10	4.5	-0.4	25	-9
2022	17.2	10.1	3.3	34	-9

Table 7 Temperature observation for period of 6 month before bridge measurements

Year	Avg Max [O]	Avg Mean [O]	Avg Min [O]	Max [O]	Min [O]
2017	26.9	19.2	11.4	40	-3
2020	15.6	9.2	3.5	34	-9
2022	13.6	7.5	1.66	34	-10

Tables 5 to 7 show the ambient temperatures for 2017, 2020 and 2022. The temperature was studied for three periods of 1, 3 and 6 months before the measurements. For a period of 6 months, the average mean temperature for 2017 is 19.2°, while for 2020 and 2022 it has dropped to around 7.5-9.2°. For a period of 3 months, the average mean temperature is different for each year, where for 2017 it is 20.5°, for 2020 it is 4.5° and for 2022 it is 10.1°. For a period of 1 month, the average mean temperature for 2017 and 2022 is around 15.5°, while for 2020 it has dropped to 6.5°.

Fig. 9 show the temperature observation over past six months before bridge measurements: maximum daily values, minimal daily values, and average daily data.

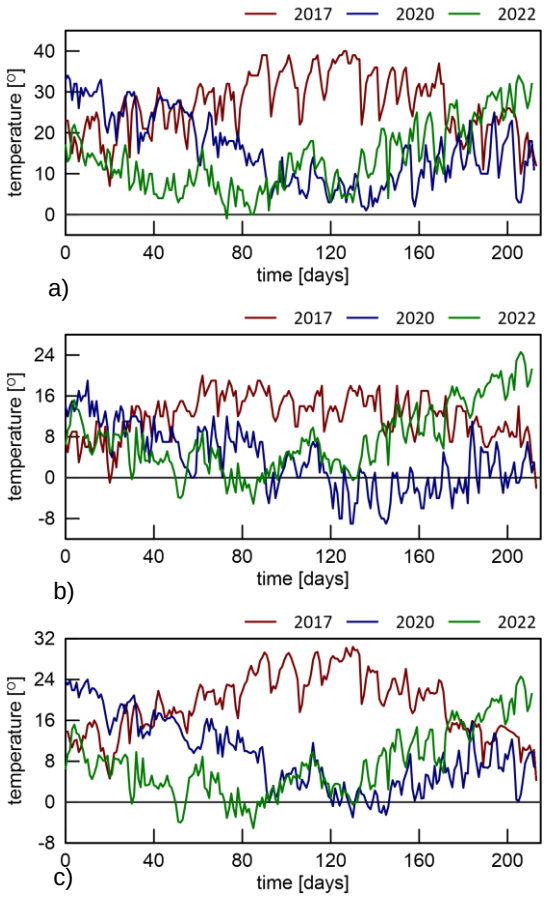

Figure. 9 Temperature observation over past six months before bridge measurements
a) Maximal daily values b) Minimal daily values c) Average daily data

Fig. 10 shows the maximum (red line), minimum (blue line) and average temperatures (grey) in ◦C, of the location in the period of the construction of the bridges to the end of the May, 2022, when the last measurements of the bridges were performed. Fig. 10 b) presents the temperature the air needs to be cooled to (at constant pressure) to achieve a relative

humidity (RH) of 100% (source: www.wunderground.com).

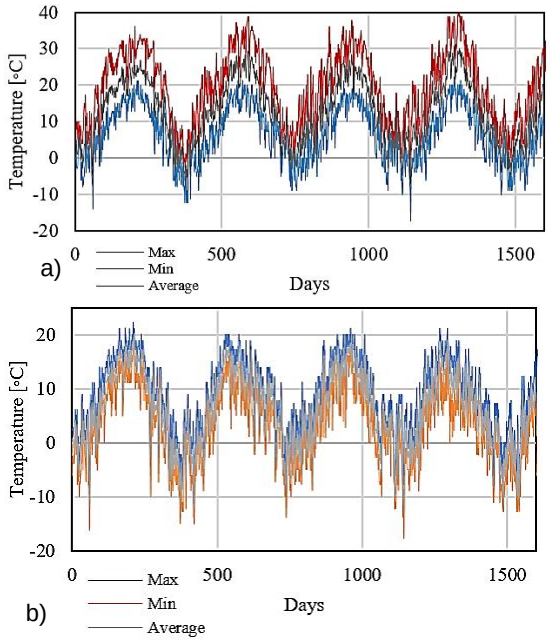

Figure 10. Maximum, minimum and average temperatures on the location, b) dew point values for the period of existing the structures. *Source: www.wunderground.com*

3.2 HUMIDITY

In addition to the analysis of the ambient temperature, an observation of humidity was also performed for a period of 1, 3 and 6 months before the measurement of the bridges. The results of this observation are shown in Table 8 through the average of daily maximum values. The average of daily maximum humidity for a period of 6 months is in range of 87.7%, 92.4% and 91.9%. In the case of a period of 1 month the average of daily maximum humidity is almost constant between 91.8% and 92.1%.

Table 8 Mean humidity of maximum daily values

Observation Period [months]	Average of daily maximum values [%]		
	2017	2020	2022
1	92.1	91.8	91.95
3	85.3	92.9	90.0
6	87.7	92.4	91.9

The maximum, minimum and average humidity on the location in the period of existing the structures, almost 5 years, (1.1.2017-31.5.2022) is presented on Fig. 11. This figure shows that the average humidity during the whole period is almost 70%.

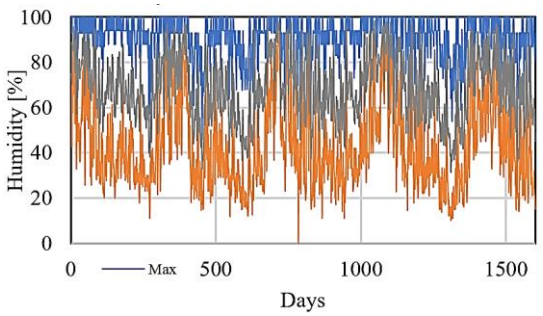

Figure 11. Maximum, minimum and average humidity [%] on the location
Source: www.wunderground.com

3.3 WIND SPEED

Wind speed is the characteristics of air movement that can have influence of the dynamic characteristics of bridge structures, especially of long span bridges. The wind conditions have no significant influence of the considered reinforced concrete frame bridges, but it is taken into account in this investigation. Herein, only maximum and average wind speed at the location is presented in the period of bridges existence (Fig. 12).

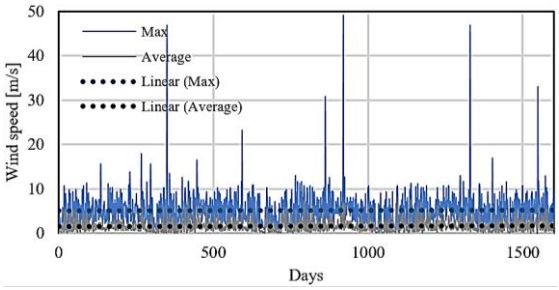

Figure 12. Wind speed at the location of bridges
Source: www.wunderground.com

From the Fig. 12 it can be concluded that on the location of the bridges, the maximum wind speed is almost 50 m/s, but the average speed is 1.5m/s.

4. CONCLUSIONS

The objective of this study is to investigate the environmental effects on the dynamic characteristics of two base-isolated highway monolithically constructed frame overpasses. The dynamic characteristics of the structures are defined using large scale ambient vibration testing. To consider the difference in the dynamic characteristics of the structures, three measurements were performed to both bridges. The first measurements were realized after the construction of the structures, in 2017; second one 3 years later, in 2020; and the last one 2 years after the second measurements, in 2022.

The ambient vibration tests were conducted under the environmental excitations in the bridges and the dynamic characteristics of structures were accurately extracted. Both overpasses were exposed on only environmental atmospheric conditions. They are still not in use, so they were no exposed-on service loads. From the obtained results and the environmental investigation, it can be stated that:

- There are differences in the results from the performed ambient vibration testing in three periods of the existing the structures. Since they are not in use and are no exposed to service loads, it can be concluded that the environmental conditions have influence of the dynamic characteristics of the structures.
- The natural frequencies of both structures are higher with the time. Especially in longitudinal and transversal directions. The difference in vertical direction is almost the same.
- The difference between the measured frequencies from first two measurements is bigger than the second and the third measurement, that means that the structure is getting stabilized.
- Temperature and humidity have influence of the dynamic characteristics of the structures.
- Wind speed do not have influence of the dynamic characteristics of the structures.

REFERENCES

[1] Li, H., S. Li, J. Ou, and H. Li. 2010b. “Modal identification of bridges under varying environmental conditions: Temperature and wind effects.” Struct. Control Health Monit. 17 (5): 495–512.

[2] Kulprapha, N., and P. Warnitchai. 2012. “Structural health monitoring of continuous prestressed concrete bridges using ambient thermal responses.” Eng. Struct. 40 (Jul): 20–38.

[3] Zhou, G.-D., and T.-H. Yi. 2014. “A summary review of correlations between temperatures and vibration properties of long-span bridges.” Math. Prob. Eng. 2014: 1–19. https://doi.org/10.1155/2014/638209.

[4] Lu, Z. R., and S. S. Law. 2006. “Identification of prestress force from measured structural responses.” Mech. Syst. Sig. Process. 20 (8): 2186–2199.

[5] Cook, R. D., D. S. Malkus, M. E. Plesha, and R. J. Witt. 2001. Concepts and applications of finite element analysis. 4th ed. New York: John Wiley & Sons.

[6] Siddique, A. B., B. F. Sparling, and L. D. Wegner. 2007. “Assessment of vibration-based damage detection for an integral abutment bridge.” Can. J. Civ. Eng. 34 (3): 438–452.

[7] Domaneschi, M., M. P. Limongelli, and L. Martinelli. 2013. “Vibration based damage localization using MEMS on a suspension bridge model.” Smart Struct. Syst. 12 (6): 679–694.

[8] Xia, Q., J. Zhang, Y. Tian, and Y. Zhang. 2017. “Experimental study of thermal effects on a long-span suspension bridge.” J. Bridge Eng. 22 (7): 04017034.

[9] Asadollahi, P., and J. Li. 2017. “Statistical analysis of modal properties of a cable-stayed bridge through long-term wireless structural health monitoring.” J Bridge Eng. 22 (9): 04017051.

[10] Moser, P., and B. Moaveni. 2011. “Environmental effects on the identified natural frequencies of the Dowling Hall Footbridge.” Mech. Syst. Sig. Process. 25 (7): 2336–2357.

[11] Giraldo, D. F., S. J. Dyke, and J. M. Caicedo. 2006. “Damage detection accommodating varying environmental conditions.” Struct. Health Monit. 5 (2): 155–172.

[12] Zhou, S. L., and W. Song. 2017. “Environmental-effects-embedded model updating method considering environmental impacts.” Struct. Control Health Monit. 25 (3): e2116.

Zlatko Srbinoski
PhD, Full Professor
Ss. Cyril and Methodius University in Skopje
Faculty of Civil Engineering
N. Macedonia
srbinoski@gf.ukim.edu.mk

ON THE OCCASION OF THE 80TH BIRTHDAY OF PROFESSOR RISTO RIBAROSKI

OVERVIEW ON THE SCIENTIFIC AND ACADEMIC CONTRIBUTION OF PROFESSOR RISTO RIBAROSKI WITH EMPHASIS ON HIS PUBLICATIONS

Prof. Ribaroski has abundant, versatile and significant opus. While he was one of the few in geodesy professors in Macedonia, teaching many generations of students in geodesy and other subjects in geodetic-civil engineering fields, he was also able to write and publish textbooks in almost all subjects he was teaching. Many of those are the first ever textbooks in Macedonia in the relevant subjects. Prof. Ribaroski was also leading and participating in many scientific projects which were presented at international events. Some biographic data about Prof. Ribaroski are presented below.

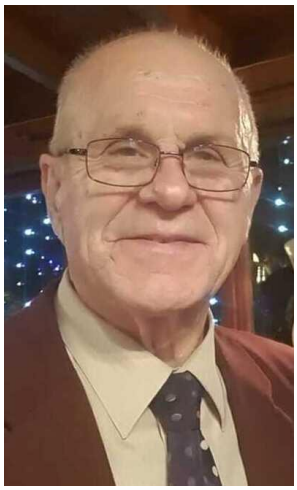

Prof. Ribaroski was born in Bucharest (Romania) in 1943, in a family of Macedonian emigrants. He spent his childhood and youth in Ohrid, Skopje and Belgrade – elementary education was completed in Ohrid, Civil engineering high school (geodesy department) in Skopje and University education at the faculty of civil engineering in Belgrade. At 1969, he started working at the Faculty of Civil Engineering in Skopje (St. Cyril and Methodius University) and progressed to be assistant

professor in 1979, associate professor in 1984 and full professor in 1990.

The job description at the Faculty included theoretical and on-field practices with the students of civil engineering and architecture. Also, he lectured geodesy and practical geodesy on part-time basis in the period 1973-75 at the civil engineering high school in Skopje. Mr. Ribaroski spent the summer semester in 1977/78 at the Geodesy institute of the Civil Engineering Faculty in Bucharest (Romania), where he got familiar with the latest geodesy achievements at that time and prepared his habitation work - *Theoretical aspects of preparing stenographic projection of the territory of Republic of Macedonia*.

After being elected as university lecturer assistant professor in 1979, Mr. Ribaroski lectured the following subjects: theory of errors with adjustments, geodetic calculations, basics in high geodesy, and geodesy for the students of first level in geodesy, as well as geodesy for students of civil engineering study programme at all departments of the Faculty of Civil Engineering in Skopje.

After the establishment of the full Geodesy studies in year 2001, prof. Ribaroski lectured the following subjects: theory of errors, high geodesy, combined parametric-correlative adjustments, and management and technology of geodetic works. Between 1995 and 2003, he lectured also the following subjects at the Faculty of Geology and Mining at the Goce Delchev University in Stip: geodesy and surveying in mining to the students from the mining department and subject maps and geomorphology to the students from the geological department.

Upon establishment of the Military Academy in Skopje, prof. Ribaroski lectured applicative geodesy with GIS for three years. Also, he lectured cartography at the post-graduate studies at the Faculty of natural sciences and mathematics in Skopje until his retirement in 2007. And after the retirement, in the period 2010-2017, he lectured geodesy, basics on civil engineering and civil engineering in mining at the University Goce Delchev in Shtip - Faculty of Natural and Technical Sciences.

Prof. Ribaroski started to publish textbooks in 1988, when his first textbook *Theory of errors with adjustments* was published by the Ss.Cyril and Methodius University – Skopje. In that textbook, calculating and adjustment of direct, indirect and conditional measurements are presented in clear and explicit way. By providing many examples, those subjects are in fact understandable to all readers.

In 1994, the University of Cyril and Methodius published Prof. Ribaroski's 2nd book – *Basics of high geodesy*. This is original and specific textbook, since it comprises subjects such as mathematical cartography, geodetical astronomy, precise geodetical measurements, satellite positioning etc. This textbook presented all modern achievements of the Geodetical science at that time.

After the first edition of the first textbook *Theory of errors with adjustments* was sold out, the 2nd edition was prepared in 1997. This edition was adjusted to the needs of the upcoming geodesy studies which started in 2001. Apart from the content from the first edition, the 2nd edition was enriched with theory of probability elements in theory of errors.

The next textbook was published in 1999 under the subject *Geodetic calculations*, as per the program that included this subject in the final semester of the Geodesy studies. This textbook was about practical application of indirect and conditional adjustments to certain geodetic points and smaller networks. The numerous examples presented in explicit way enabled easier understanding of this complex subject which has mathematical backgrounds from Theory of errors with adjustments. With this textbook, Prof. Ribaroski completed his opus for all subjects he was teaching at the first-degree geodesy studies at the Faculty of Civil Engineering in Skopje.

Prof. Ribaroski's next textbook– *Practical Geodesy*'was published in 2003 by the Faculty of Civil Engineering in Skopje. This textbook was adjusted to the program of all departments of civil engineering studies and apart from the usual geodesy content, it contained parts about the modern methodologies at that time. It was therefore considered a modern textbook that presents all the benefits from the modern geodesy practice methodologies to the readers.

As a contribution to the newly-started complete geodesy studies at the Faculty of Civil Engineering in Skopje, Prof. Ribaroski published the textbook *High geodesy – Basic geodetic networks* in 2005. This textbook contains the three basic parts of High geodesy: existing basic geodetical networks (one and two-dimensional), precise geodetical measurements that are applied during establishment and maintenance of the basic geodetical networks and special (global, three-dimensional) geodetical networks as a new

modern, reality. This textbook is original piece in Macedonian language.

During same year, Prof. Ribaroski also published the textbook *Management and technology of the geodetical works* which is used by the geodesy students at the Faculty of the civil Engineering. The main moto of this textbook is that – 'The economic activity consists of people, products and profit, but the most important element are the people' (Lee Iacocca).

Just before his retirement, in 2007, Prof. Ribaroski published his most complex textbook – *Combined parametric – corelative adjustments*. Although it is mainly intended to be used for the post-graduate geodesy studies, this textbook can be useful to the geodesy experts for resolving numerous practical theoretical issues during the every-day geodesy practice.

Following the retirement, Prof. Ribaroski published two more handbooks for the students of the Goce Delchev University in Shtip – *Geodesy* in 2014 and *Civil Engineering in Mining* in 2017. Both are available in digital format as part of the e-library of the Goce Delchev University in Shtip.

To conclude, Prof. Ribaroski's publishing activity is abundant, versatile and continuous. All his textbooks are using simple expressions, enabling the readers to easily apply the content in their everyday practice. One of the main benefits from Prof. Ribaroski's textbooks is establishing original terminology in Macedonian language for numerous technical expressions and procedures that were non-existing due to the small number of specialized geodesy textbooks published in Macedonian language.

Apart from the educational activities, Prof. Ribaroski also had success in offering expert advices. It is usual for the professors from the faculty of civil engineering to cooperate with different corporate entities and other specialized organizations by offering expert advice and solutions for different types of complex problems. Prof. Ribaroski was included in such activities from the very beginning of his career as assistant professor and to date has participated in about 150 such projects, either as individual or as a team member. Those project activities include geodetic measurements, calculations, adjustments, and above all numerous examinations of the stability of different objects of capital significance for the country. As result of such activities, many studies, projects and audits were produced, most of which under direct supervision of Prof. Ribaroski.

Prof. Ribaroski also had success in the field of Science. He participated in many congresses, seminars and symposiums and was also managing several scientific projects, out of which two are most significant. Under his leadership, the scientific Project – *Choosing the most suitable cartographic projection for the presentation of the territory of Republic of Macedonia* was completed in 1998. After that, in 2003, the project *Applying the UTM projection and WGS geodetical system as basic NATO standards in the cartographic projection of Republic of Macedonia* was completed. With these two projects, all problems regarding the compliance of our basic standards with the European and world standards were theoretically resolved.

Looking at Prof. Ribaroski's opus, it can be confirmed that small nations do big things, i.e. there are numerous scientists and educators from less developed countries that have significant achievements during their careers, which leave everlasting mark in their direct and wider surrounding.

SJCE

SCIENTIFIC JOURNAL OF CIVIL ENGINEERING

SS CYRIL AND METHODIUS UNIVERSITY
FACULTY OF CIVIL ENGINEERING